

PHOSPHORUS CHEMISTRY AND RELEASE IN RESTORED AND AGRICULTURAL FLOODPLAINS AFTER FREEZING AND THAWING

by

Shannon K. Donohue

A Thesis

Submitted to the Faculty of Purdue University

In Partial Fulfillment of the Requirements for the degree of

Master of Science



School of Agricultural and Biological Engineering

West Lafayette, Indiana

May 2021

THE PURDUE UNIVERSITY GRADUATE SCHOOL
STATEMENT OF COMMITTEE APPROVAL

Dr. Sara McMillan, Chair

School of Agricultural & Biological Engineering

Dr. Gregory Noe

United States Geological Survey

Dr. Mark Williams

U.S. Department of Agriculture – Agricultural Research Service

Approved by:

Dr. Linda Lee

Dr. Nathan Mosier

*Dedicated to my siblings for understanding and supporting me as perhaps few others could—
Mom would be proud.*

ACKNOWLEDGMENTS

I would like to acknowledge my advisor, Dr. Sara McMillan and committee members Dr. Greg Noe and Dr. Mark Williams for their continued guidance and patience throughout this process. I could not have done this without the help of the entire EBOW lab, specifically Dani Winter, Ariana Montoya, Mandy Limiac, and all the undergrads. I also would like to acknowledge the lab technicians at the NSERL for training on the instruments. This research was made possible with funding from NSF and the Purdue Graduate School David M. Knox fellowship.

TABLE OF CONTENTS

TABLE OF CONTENTS.....	5
LIST OF TABLES	8
LIST OF FIGURES	9
LIST OF ABBREVIATIONS.....	10
ABSTRACT.....	11
1. P CHEMISTRY AND RELEASE IN FLOODPLAIN SOILS AFTER FREEZING AND THAWING	12
1.1 Introduction	12
1.2 Literature Review.....	14
1.2.1 The Phosphorus Cycle	14
1.2.2 Importance of Floodplains to P Cycling	15
1.2.3 Freeze-thaw Cycles	17
1.2.4 Freeze-Thaw and Phosphorus	18
1.3 Methods.....	21
1.3.1 Location	21
1.3.2 Experimental Design.....	22
1.3.3 Experiment 1: Potential Impact of Freezing and Thawing on Soil Extractable Metals & Phosphorus.....	23
Sequential Phosphorus and Metal Extractions.....	24
1.3.4 Experiment 2: Phosphorus Release to Surface Water Following Flooding Compared to Flooding after Freeze-Thaw.....	25
Flood Microcosm Incubations	25
Phosphorus and Metal Extractions.....	26
1.3.5 Soil Physicochemical Characteristics	27

1.3.6	Statistical Analyses	27
1.3.7	Experiment 1: Potential Impact of Freezing and Thawing on Soil Extractable Metals & Phosphorus.....	28
1.3.7.1	Experiment 2: Changes in Phosphorus Release During Flooding After FT	28
	Drivers of Phosphorus Release at Important Timepoints (4 days, 8 days, 14 days).....	28
	Sequential Extraction Phosphorus Pools and Metals.....	30
1.4	Results	30
1.4.1	Experiment 1: Potential Impact of Freezing and Thawing on Soil Extractable Metals & Phosphorus.....	30
	Freezing Effects on Extractable Phosphorus	30
	Freezing Effects on Extractable Metals	31
1.4.2	Experiment 2: Phosphorus Release to Surface Water Following Flooding Compared to Flooding after Freeze-Thaw.....	32
	Flooding and FT Effects on Extractable Phosphorus	32
	Flooding and FT Effects on Metals	33
	Freezing and Thawing Treatment Effect on P Release.....	34
	Drivers of Phosphorus Release	35
1.5	Discussion	37
1.5.1	Experiment 1: Potential Impact of Freezing and Thawing on Soil Extractable Metals & Phosphorus.....	37
	Freezing Effects on Extractable Phosphorus	37
	Freezing Effects on Extractable Metals	38
1.5.2	Experiment 2: Phosphorus Release to Surface Water Following Flooding Compared to Flooding after Freeze-Thaw.....	39
	Flooding and FT Effects on Extractable Phosphorus	39
	Flooding and FT Effects on Extractable Metals	40

Freezing and Thawing Effect on Phosphorus Release.....	40
Drivers of Phosphorus Release	41
1.6 Conclusions	47
APPENDIX A. PHOSPHORUS EXTRACTION SCHEME	49
APPENDIX B. SUPPLEMENTAL DATA	50
REFERENCES	52

LIST OF TABLES

Table 1 Starting water chemistry for flood incubations where nutrient measurements were taken before flooding and temperature, dissolved oxygen, and pH were measured 2 hours after the onset of flooding..... 35

Table 2- Mean physicochemical properties by site measured pre-flooding. Where, BD= bulk density; OM=organic matter; MC= moisture content; TEP= Total Extractable P; T. Ext= total extractable; WR-A = Wabash R. Agriculture; WR-M = Wabash R. Mitigation; TR-P 36

LIST OF FIGURES

Figure 1 Inorganic and organic pools of P, transformations are represented by dotted arrows. Grey circles represent extractions run on soils during the experiment to quantify each pool.	15
Figure 2 Map of floodplain sampling sites along the confluence of the Wabash and Tippecanoe Rivers in Indiana, USA.	21
Figure 3 Experimental design scheme, where boxes represent samples and arrows represent a full P-extraction scheme conducted on soils (detailed extraction scheme in Appendix A).	23
Figure 4- Total extractable P (TEP) in mg g ⁻¹ Dweq soil from sequential P extractions and the mean proportion of each pool within TEP. Bars represent one standard deviation (SD). Letters represent significant differences between treatments.	31
Figure 5- Mean extractable metals reported in mg/g Dweq soil. Bars represent 1 standard deviation. Letters indicate significant differences between samples as indicated by p-values of Wilcoxon signed-rank tests run on paired samples.	32
Figure 6 Median SRP (mg) released in control and treatment cores by each sampling timepoint. Points represent individual cores. P-values obtained from Wilcoxon signed-rank tests.	34

LIST OF ABBREVIATIONS

Al	Aluminum
Amox	Ammonium Oxalate
BD	Bulk Density
BMP	Best Management Practice
Ca	Calcium
CaCO ₃	Calcium Carbonate
DCB	Dithionite-Citrate-Bicarbonate
DO	dissolved oxygen
DOC	Dissolved organic carbon
DON	Dissolved organic nitrogen
Dweq	Dry weight equivalent
Fe	Iron
FT	Freeze-thaw
HCl	Hydrochloric acid
M	Mean
MC	Moisture Content
Mdn	Median
Mn	Manganese
N	Nitrogen
NaOH	Sodium hydroxide
NRP	Non-reactive P
OM	Organic Matter
P	Phosphorus
SRP	Soluble-reactive P
T. Ext	Total Extractable
TEP	Total Extractable P
TP	Total P

ABSTRACT

Disturbance regimes like freezing and thawing (FT) can have potentially significant impacts on nutrient release from soil and are predicted to increase with climate change. This is particularly important in biogeochemical hotspots like floodplains that can both remove and release nutrients to surface waters during flooding. Connection between the river and floodplain can improve water quality by reducing nutrient loads through microbial processes and sedimentation. However, conditions during flooding can also lead to phosphorus (P) release from pools that are not normally bioavailable. Disturbance events like FT can also lead to changes in bioavailable P due to microbial cell lysis. This study investigates differences in P chemistry and flux during flooding from intact soil cores that have undergone a FT cycle compared to soils that have not undergone freezing. Floodplain soils were collected from four sites along the Wabash and Tippecanoe Rivers in Indiana. We hypothesized that (i) the primary pools of P within the soil would change with freezing (ii) and flooding; (iii) frozen treatment cores would release more P during flood incubations than unfrozen control cores; and (iv) processes controlling P release during flood incubations would change after FT due to changes in the primary pools of P in the soil cores.

On average, soil cores that underwent FT released greater amounts of P than unfrozen cores over the course of the 3-week experimental flood incubation. Phosphorus release in both unfrozen control and FT treatment cores during flooding was explained in part by soil extractable Al and Fe and redox status; however, P release was influenced by soil Ca-P in the FT cores to a greater extent than unfrozen cores. Phosphorus release in FT cores occurred faster than in control cores with overlying water concentrations peaking 2 weeks after onset of flooding, followed by lower concentrations at 3 weeks. Whereas control cores had some release and uptake early on but then released P throughout the 3-week incubation—supporting the hypothesis that drivers of P release were different after FT. Interactive effects of FT and flooding suggest that concentration gradients between soil pore water and overlying surface water could have enhanced dissolution of the Ca-P pool, highlighting the importance of floodwater chemistry to P dynamics following FT. This study provides an important link between observed winter floodplain P loss and potential drivers of release and retention, which is critical to informing floodplain restoration design and management through all seasons.

1. P CHEMISTRY AND RELEASE IN FLOODPLAIN SOILS AFTER FREEZING AND THAWING

1.1 Introduction

Freshwater systems experience eutrophication that can lead to harmful algal blooms, impairing water quality and human health. Most often, phosphorus (P) is the limiting nutrient in these systems, with excess P loads coming from point and non-point sources. Agricultural systems in the Midwestern United States are a major non-point source of nitrogen (N) and P to surface waters, which has prompted land managers to implement innovative solutions to avoid nutrient loss. Best management practices (BMPs) including cover crops, no-till farming, floodplain restoration, and wetland restoration that may reduce N loads and soil erosion, can inadvertently increase P loads (Surridge et al., 2012; Christian et al., 2009; Messiga et al., 2010; Liu et al., 2019). Hydrologic connectivity between rivers and floodplains has important implications for nutrient retention (Junk et al. 1989; Tockner et al., 1999). Floodplain reconnection can improve overall water quality by decreasing in-channel erosion and reducing nutrient loads via sedimentation, uptake, and microbial processes. However, prolonged inundation and reducing conditions during flooding can cause P that is normally not bioavailable to be released into the water column via dissolution of redox sensitive Al and Fe oxides (Wright et al., 2001; Christian et al., 2009), or dissolution of Ca-P in more calcareous soils (Jayarathne et al., 2016; Weihrauch & Opp 2018).

Disturbance regimes like drying-rewetting and freezing and thawing (FT) have the potential to increase nutrient losses to surface waters via the lysis of microbial cells, shearing of particle surfaces, cracking and other changes in terrestrial soils (Blackwell et al., 2010). Suppressed microbial activity can limit reassimilation of nutrients post-disturbance, and re-establishment of the microbial pool after freezing has been shown to take longer than after drying (Yevdokimov et al., 2016). In some settings, studies suggest that freezing will not have a significant impact on P release under cold flooding conditions typical of spring thaw periods due to lower redox potential (Eh) compared to flooding under warmer conditions (Kumaragamage et al., 2020). In a study looking at P transformations in Chinese forest and grassland soils, no significant differences were found in total extractable P or P fractions after FT treatment of soils (Xu et al., 2011). While still, others have found that FT cycles can increase bicarbonate extractable inorganic and organic P in

soils, with the greatest impacts occurring after 1-2 FT cycles and diminishing with additional cycles (Sun et al., 2019). In some alpine soils, total dissolved P following a single FT cycle significantly increased, with much of the P associated with the dissolved organic fraction (Freppaz et al., 2007). Additional FT cycles in these soils did not lead to additional changes, though others have found contrasting results. Ron Vaz et al. (1994) found that increasing the number of FT cycles increased TDP in organic soils but had opposite effects in mineral soils, and that speed of freezing positively correlated with nutrient release. In addition to riparian soils, in-stream sediments can be affected by FT as daily FT cycles can break down particles and organic matter, leading to competition for sorption sites and increasing P release (Liao et al., 2019). These sometimes inconsistent patterns have raised questions about the influence of FT on P loads under various environments and conditions.

Studies have shown that agricultural BMPs like cover crops (Liu et al., 2019), no-till management (Messiga et al., 2010), and tile drainage (King et al., 2015) aimed at improving water quality via reductions in erosion and N via denitrification can lead to increased P losses. Despite seasonal freezing in the northern hemisphere, and much of the annual P load in agricultural watersheds occurring during the cold non-growing season, there is little understanding of the influence of FT on nutrient release in river-floodplain systems. The influence of FT on P is supported by evidence of high total P (TP) loads from watersheds during spring melt (thawing) that is often, but not always discharge dependent, suggesting in-soil or in-stream conditions can play a role (Casson et al. 2019; Good et al., 2019). Under future climate scenarios FT cycles are predicted to increase (Henry et al., 2008), highlighting the need for this area of research.

This study aims to quantify the potential for increased P release during floodplain inundation following a single FT cycle. We hypothesized that (i) the primary pools of P within the soil would change with freezing (ii) and flooding; (iii) more P would be released from soils during flooding following FT due to the lysis of microorganisms and mineralization of organic matter during freezing; and (iv) processes controlling P release would change after FT due to changes in the primary pools of P in soil.

1.2 Literature Review

1.2.1 The Phosphorus Cycle

Phosphorus is an essential nutrient that is an element in the DNA and other essential molecules of organisms and is often the limiting nutrient in freshwater ecosystems. Excess P in runoff or subsurface leaching from point and non-point sources can lead to increased eutrophication and harmful algal blooms (Arenberg & Arai, 2019; Bennet & Schipanski, 2012). Land use practices can play an important role in reducing excess P in runoff, which is why understanding P dynamics in a variety of soil types under all environmental conditions is important.

The primary source of soil P is the weathering of bedrock apatite minerals containing phosphate linked by calcium ions (Figure 1). In a fully developed soil, P will have been weathered from the bedrock apatite minerals into a form of phosphate (PO_4^-). Phosphate chemically binds or adsorbs to humic substances, clays, and metal oxides, which results in pools of P that move physically with the soil and are largely not bioavailable (Filippelli, 2019; Bennet & Schipanski, 2012). Phosphorus cycling in soil systems happens at various time scales. Soluble P defined as P in solution, is quickly recycled as labile P, taken up by organisms in the form of orthophosphate, temporarily sorbed to binding sites, or lost to leaching. Alternatively, transformations from soluble to occluded P require geologic timescales (Smeck, 1985). If the soil solution becomes undersaturated with primary minerals like apatite, or secondary P minerals like carbonates or Fe and Al oxides, mineral dissolution or desorption can occur (Smeck, 1985). Undersaturation can occur as the result of subsurface leaching or losses to overlying surface water.

Refractory pools, or pools that are not readily bioavailable, include P within apatite minerals, and P adsorbed or co-precipitated onto Al, Fe, and Mn oxyhydroxides (Bennet & Schipanski, 2012). The least available form is occluded P, which is P physically encapsulated by minerals (Smeck, 1985). When inorganic P is introduced to a system, such as after fertilizer application, it can be adsorbed onto positively charged soil surfaces including metal oxides, clays, and certain minerals. Desorption is largely dependent on pH and redox conditions. To speed up the transformation of P and increase the availability of orthophosphate, plants and microbes will secrete phosphatase enzymes that decompose organic P to orthophosphate (Filippelli, 2019; Weihrauch & Opp, 2018;

Hoffmann et al., 2009). As P becomes available, plants and organisms will incorporate it into their biomass, decomposition of organic litter will result in a variable pool of organic P.

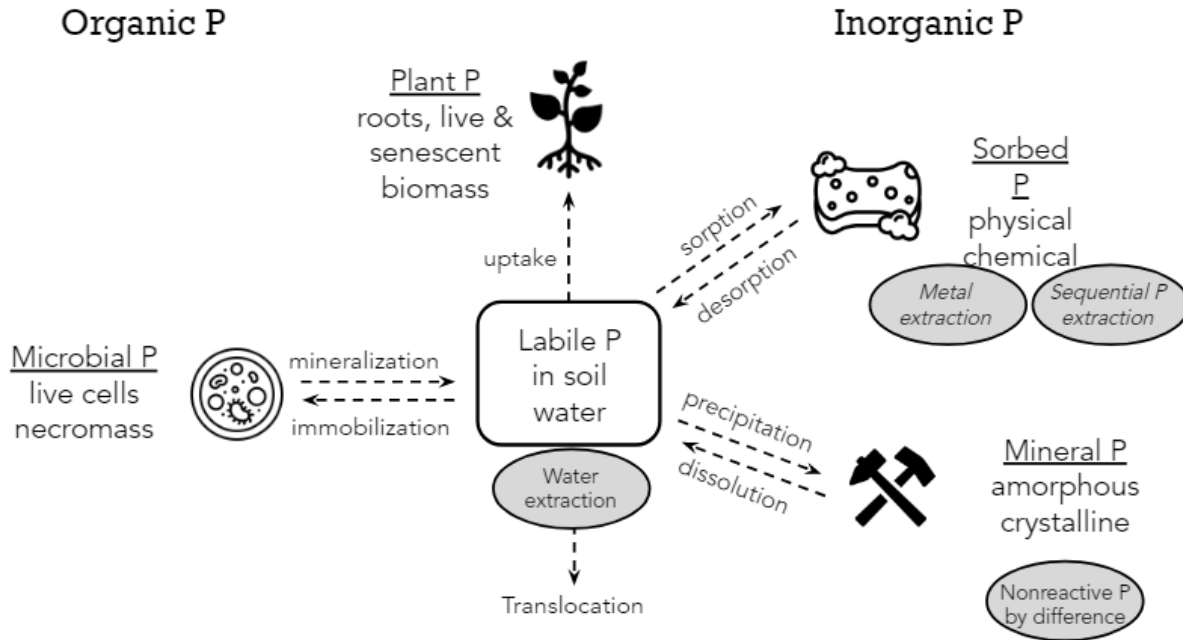


Figure 1 Inorganic and organic pools of P, transformations are represented by dotted arrows. Grey circles represent extractions run on soils during the experiment to quantify each pool.

Labile P pools include dissolved phosphate ions in solution and P incorporated into dissolved organic matter (Bennet & Schipanski, 2012). Organic P occurs mainly as ester linkages on inositols with smaller fractions in phospholipids and nucleic acids, which suggests it originates from microbial synthesis rather than accumulation of plant/animal residues (Smeck, 1985). Organic P availability will depend on the rate of mineralization and biodegradability of the substrate (Reddy et al., 2000). Mineralization rates will be influenced by soil P concentrations, pH, and redox status. Changes in environmental conditions, like flooding, can lead to shifts in the distribution of P between these pools.

1.2.2 Importance of Floodplains to P Cycling

In river systems, hydrologic connectivity of the floodplain plays a strong role in sediment and nutrient retention (Junk et al. 1989; Tockner et al., 1999). Reconnecting rivers to their floodplains can reduce nutrient loads via sedimentation and microbial processes, decrease erosion, and

improve overall water quality (Noe & Hupp, 2005; Noe et al., 2019; McMillan & Noe, 2017). Restoring wetlands has similar benefits such as reduced runoff, increased nutrient retention, and in turn reduced eutrophication (Reddy et al., 2000; Wolf et al., 2013). Restoration of former agricultural lands to wetlands and reconnection of floodplains to surface waters are common mitigation techniques for these reasons. However, studies have shown that environmental practices that promote N removal can lead to higher P release, with potential release increasing over time as a result of water saturation and development of reducing conditions (Liu et al., 2019; Aldous et al. 2005; Surridge et al., 2012). A recent study by Weihrauch & Weber (2020) showed that floodplain subsoils enriched in soluble P may be a significant source of P to surface water previously unaccounted for.

During flooding, P is delivered to the soil from floodwater in both particulate and dissolved forms. Soil properties will control whether the sediment acts as a source or sink for the incoming P. If floodwater P concentrations are high, it is likely much of the P will be retained by Fe, Mn and Al oxides in acid soils, and Ca in alkaline soils (Reddy et al., 2000). If porewater P concentrations are higher than floodwater concentrations, P can diffuse to the overlying water or co-precipitate with Ca. Nutrient dynamics will change based on both biotic and abiotic factors but in P cycling, redox conditions play a critical role.

Conditions experienced during flooding can cause P that is normally not bioavailable to be released into the water column. When soils are inundated over long periods, O₂ from floodwater gets depleted by cellular respiration. This eventually leads to the formation of an anaerobic zone within the soil/floodwater forcing microbes to use electron acceptors in the order of O₂ > NO₃ > Mn (IV) > Fe (III) > SO₄²⁻ > CO₂ (Reddy et al., 2000). During this time, P can be released from the reduction and dissolution of Fe phosphates, the hydrolysis and dissolution of Fe and Al phosphates, or the release of clay-associated phosphates through anionic exchange (Wright et al., 2001). The rate and degree of Eh reduction is a microbially mediated process influenced by electron acceptors, water temperature, and other soil properties (Jayarathne et al. 2016; Kumaragamage et al., 2020).

P adsorbed to Ca minerals is not redox sensitive like P adsorbed to Fe, Al, and Mn but rather driven by pH and concentration gradients. It is often the main control on soil solution P in calcareous soils

(Jayarathne et al. 2016). Under alkaline conditions, bonds between orthophosphate and calcium become more common as Ca^{2+} exchanges H^+ protons on oxyhydroxide surfaces. This creates a monolayer of P ions on carbonates that can precipitate when soil solution P concentrations get high enough, or release orthophosphate if pH lowers (Weihrauch & Opp, 2018).

1.2.3 Freeze-thaw Cycles

Organic nutrients in soil are, in part, held within the living microbial and plant biomass. During drying, water held within the cells is released causing the cells to shrink or die. Rapid rewetting acts as a shock leading cells to burst and release the nutrients and detritus previously stored within their membranes (Aldous et al., 2005; Baldwin & Mitchell, 2000; Blackwell et al., 2010), reducing microbial abundance while providing new substrates and metabolites for surviving organisms to use. Freezing and thawing (FT) behaves similarly; as water freezes it expands which can also lead to the lysis of cells (Blackwell et al., 2010). Freezing and thawing along with other disturbances like drying rewetting have shown to influence C and N solubilization (Gao et al., 2018; Matzner & Borken, 2008), but less is known about the effect on P (Song et al., 2017; Blackwell et al., 2010; Freppaz et al., 2007; Vaz et al., 1994). One study by Yevdokimov et al. (2016) showed that freezing had a stronger effect on P release than drying due to a slower re-establishment of the microbial pool after freezing. Suppressed microbial activity can thereby limit the reassimilation of P after disturbance. The influence of FT on P is supported by evidence of high total P (TP) loads from watersheds during spring melt (thawing) that is not always discharge dependent, suggesting in-soil or in-stream conditions can play a role (Casson et al. 2019; Good et al., 2019).

Freeze-thaw cycles can be particularly disruptive because in addition to lysis from the expansion of intracellular fluid, cells can be sheared by ice crystals that form within the soil pore space (Blackwell et al., 2010). The degree of soil disruption following freezing will be partially dependent on the particle size. Water held within soil clay particles often remains as bound water, leading to less cracking and fragmentation of the soil compared to coarser particles (silt or larger) which allow more ice crystals to form (Zhang et al., 2016). Similarly, the water content of the soil will influence the amount and size of soil ice crystals. Water expansion during freezing changes the structure of the soil by breaking up soil aggregates, which can release previously physically protected carbon and nutrients to the system (Sharma et al. 2006; Blackwell et al., 2010; Zhang et

al. 2016). Alternatively, shearing of the particle surfaces can result in exposure of new reactive surfaces, allowing for new binding and a decrease in the nutrient availability (Freppaz et al., 2007; Liao et al., 2019). While aggregates can be broken during the initial stages of freezing, over time smaller particles can re-aggregate and improve the soil structure after multiple FT cycles (Zhang et al., 2016).

Biomass within the soil will have different thresholds of solubilization depending on the rate, duration, and number of FT cycles which will influence nutrient release; though one cycle is usually enough to kill the less resilient organisms (Blackwell et al., 2010; Yevdokimov et al., 2016). A review on the influence of FT on the soil microbial biomass by Blackwell et al. (2010) found that in addition to type of organism, the metabolic rate of organisms can impact their response. Those in a resting state appear less susceptible to disturbances than rapidly growing organisms. Studies showed that community shifts are possible in places that experience frequent disturbances, but short-term disturbances will shift the microbial community toward a population with less active, more mature organisms.

Solubilization of P from the biomass does not necessarily mean that P will be transferred from the soil to surface waters. P released from the microbial biomass can react and adsorb to soil mineral surfaces or get assimilated by surviving microbes (Hoffman et al., 2009; Liu et al., 2019). For example, researchers observed increased P in the porewater of the Oa horizon was largely removed before leaching to the Bs horizon in forested soils (Fitzhugh et al., 2001). Delivery of P from the soil to overlying surface water will be influenced by the soil structure, vegetation status, small scale hydrologic factors and microbial spatial distribution (Blackwell et al. 2010).

1.2.4 Freeze-Thaw and Phosphorus

Phosphorus losses during the non-growing season in agricultural fields are often higher than during the growing season and account for a significant portion of annual P loads (King et al., 2015; Good et al., 2019). These loads are often discharge dependent and associated with one or several peak discharge events resulting from snowmelt or precipitation (King et al., 2015; Royer et al., 2006; Van Esbroeck et al., 2017; Williams et al., 2016). Though some studies in Canada have found variation in P loads not associated with discharge (Casson et al., 2019). Dissolved P losses

associated with subsurface flow can be enhanced by preferential flow paths in tile-drains (King et al., 2015) and in tile-drained agricultural fields, annual subsurface discharge can exceed surface discharge (Pease et al., 2018; Plach et al., 2019; Royer et al., 2006). However, surface runoff can be a significant pathway for dissolved P during wet years when overland flow is prevalent, especially following spring fertilizer application (Royer et al., 2006). Lysed plant cells from cover crops during freezing can contribute to these losses (Bechmann et al., 2005; Liu et al., 2019). Particulate P losses are predominantly associated with surface runoff and can be enhanced by rainfall on bare unfrozen thawed soil (Good et al., 2019; Van Esbroeck et al., 2017). In-stream channel erosion enhanced by freezing may also play a role in particulate P loads during the cold season (Liao et al., 2019). Dissolved and particulate P loads from leaching and overland flow will vary depending on the hydrology and antecedent conditions in the area.

Despite significant P loads occurring during colder non-growing season months, variable effects of soil freezing on P availability have been found across different settings. In some settings, studies suggest that freezing will not have a significant impact on P release under cold flooding conditions typical of spring thaw periods due to lower redox potential (Eh) compared to flooding under warmer conditions (Kumaragamage et al., 2020). In a study looking at P transformations in Chinese forest and grassland soils, no significant differences were found in total extractable P or P fractions after FT treatment of soils (Xu et al., 2011). While still, others have found that FT cycles can increase bicarbonate extractable inorganic and organic P in soils, with the greatest impacts occurring after 1-2 FT cycles and diminishing with additional cycles (Sun et al., 2019). In alpine soils, total dissolved P following a single FT cycle significantly increased, with much of the P associated with the dissolved organic fraction (Freppaz et al., 2007). Additional FT cycles in these soils did not lead to additional changes, though others have found conflicting results. Vaz et al. (1994) found that increasing the number of FT cycles increased TDP in organic soils but had opposite effects in mineral soils, and that speed of freezing positively correlated with nutrient release. In addition to riparian soils, in-stream sediments can be affected by FT as daily FT cycles can break down particles and organic matter, leading to competition for sorption sites and increasing P release (Liao et al., 2019). These sometimes inconsistent patterns have raised questions about the influence of FT on P loads under various environments and conditions.

Studies looking at P release following FT have identified environmental factors that may intensify, or mediate P loads to surface waters. Impacts of freezing on P losses can be influenced by the number and severity of freeze-thaw cycles, especially in the presence of vegetation (Bechmann et al., 2005; Henry, 2007; Messiga et al., 2010; Cober et al., 2019), though some have found impacts of FT cycles are greatest following just 1-2 cycles (Freppaz et al., 2007; Sun et al., 2019). The presence of cover crops in agricultural settings can increase dissolved reactive P losses from agricultural fields after freezing and thawing due to plant residues experiencing cell lysis, though impacts on TP losses are less clear (Liu et al., 2019; Bechmann et al., 2005). Other agricultural practices like no-till management, often used to reduce nutrient loads, have shown the ability to increase P availability and potential for leaching in soils experiencing FTCs due to the preservation of preferential flow paths (Messiga et al., 2010). Environmental factors that can mediate P released following a freeze include P sorption capacity and snow cover. Phosphorus sorption capacity of soils will influence how much P gets recycled into the soil following freezing and thawing, soils with higher sorption capacity will reduce leaching and runoff losses of P (Yevdokimov et al., 2016). Snow can act as an insulator, preventing soils from freezing even under cold conditions (Van Esbroeck et al., 2017). This will be particularly important under future climate scenarios where snow cover is predicted to decrease while frequency of extreme temperatures is predicted to increase (Henry, 2008).

Few studies have looked at the influence of freezing on nutrient retention at the land-water interface. Looking at nutrient dynamics seasonally however can provide insight to the influence of cold-season patterns. A study conducted by Satchithanatham et al. (2019) found that P dynamics were consistently controlled by abiotic adsorption-desorption over biotic factors regardless of season in flow-through riparian buffers affected by snowmelt. Water temperature during flooding can control Eh, with colder flood water temperatures typical of snowmelt releasing less P (Kumaragamage et al., 2020). However, in a field study by Noe and Hupp (2007), flooding following a freeze led to substantial release of orthophosphate and other forms of dissolved P from floodplain soils. More evidence on the influence of FT cycles in riparian areas would be useful to restoration managers looking to make the most informed decisions with future climate change scenarios in mind (Henry et al. 2008).

1.3 Methods

1.3.1 Location

This study focused on floodplains along the confluence of the Wabash and Tippecanoe Rivers near Lafayette, Indiana in Prophetstown State Park (Figure 2) ($40^{\circ} 30' 54.41''$ N; $86^{\circ} 47' 25.36''$ W). The Tippecanoe River is a major tributary to the Wabash River which begins in Western Ohio and flows southwest until it reaches the Ohio River. The entire Wabash River has a drainage area of approximately 32,500 square miles (USACE, 2007). At the confluence, the drainage area is approximately 6,346 square miles primarily composed of agriculture but also includes 10% developed land, 2.5% wetlands, and 9% forest cover. Within the entire watershed, agriculture is the predominant land use with crops like corn and soybeans accounting for approximately 62% of the land

cover (U.S. American Corp of Engineers Louisville District, 2011). The local climate is temperate with an average annual temperature of 11.2°C , ranging from approximately -6°C to 3°C during winter according to the data collected between 1981-2010 at the Purdue University airport

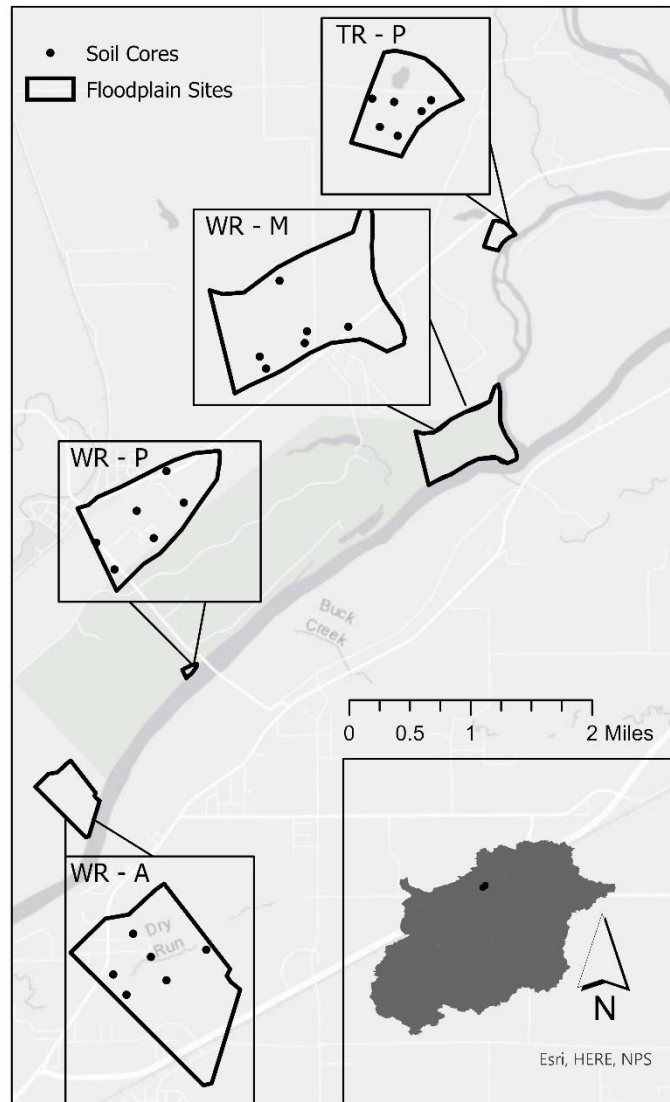


Figure 2 Map of floodplain sampling sites along the confluence of the Wabash and Tippecanoe Rivers in Indiana, USA.

weather station (Midwestern Regional Climate Center, 2020). Average annual precipitation is approximately 93 cm and mostly occurs during the spring and summer (NOAA, 2020).

To evaluate a range of possible river - floodplain connectivity conditions, four floodplain sites along the confluence of the Wabash and Tippecanoe Rivers were included in this study (Figure 2). The locations along the Wabash River consisted of a restored prairie floodplain (WR-P), an active agriculture site (WR-A), and another prairie-wetland that was recently restored as mitigation for wetland loss (WR-M). The site along the Tippecanoe River is also a restored prairie floodplain (TR-P). Restoration at prairie sites (WR-P; TR-P) converted former agricultural land through the removal and disconnection of tile drains coupled with replanting of native grasses and perennials like goldenrod. The WR-M site is 317-acres with approximately 96 acres regraded in 2010 to create more heterogeneity in the floodplain including fens and wet prairies. The site includes prairie vegetation, seasonally flooded wetlands, and ephemeral stream channels, making it the most topographically and ecologically heterogeneous site. During our sampling period, giant ragweed (*Ambrosia trifida*) dominated at the WR-M site, with native grasses remaining further from the river. Restored sites are managed by Prophetstown State Park staff through periodic controlled burns. The agriculture site (WR-A) was actively farming corn (*Zea mays*) during the growing season preceding sampling and residue remained on the soil post-harvest. Soil characteristics varied by site: well to somewhat excessively drained sandy and silty loams at WR-A; well drained silt loams at WR-M and WR-P; and well drained and very poorly drained silt and silt clay loams at TR-P as determined by the USDA NRCS web soil survey (Soil Survey Staff, 2019). Soil cores for the flooding experiment were collected at six locations representative of the range of elevations and distances from the river within each of the four sites (Figure 2).

1.3.2 Experimental Design

The study was separated into two experiments (Figure 3). Experiment 1 was designed to isolate the effect of freezing and thawing alone on soil P pools. Composite soil samples were collected from each of the 6 locations at all 4 floodplain sites using a 2.54 cm diameter soil probe to a depth of 10 cm for a total of 24 samples. Experiment 2 was designed to evaluate the effect of flooding on primary soil P pools and release in unfrozen and FT treated soils. To determine baseline pre-flood conditions, soil samples were collected using a 2.54 cm diameter soil probe to a depth of 10

cm following the same procedure as Experiment 1. In addition, intact soils cores were collected in duplicate from each floodplain location (n=24) for a total of 48 cores to be divided into unfrozen and FT treatment cores along with river water for experimental flood incubations.

1.3.3 Experiment 1: Potential Impact of Freezing and Thawing on Soil Extractable Metals & Phosphorus

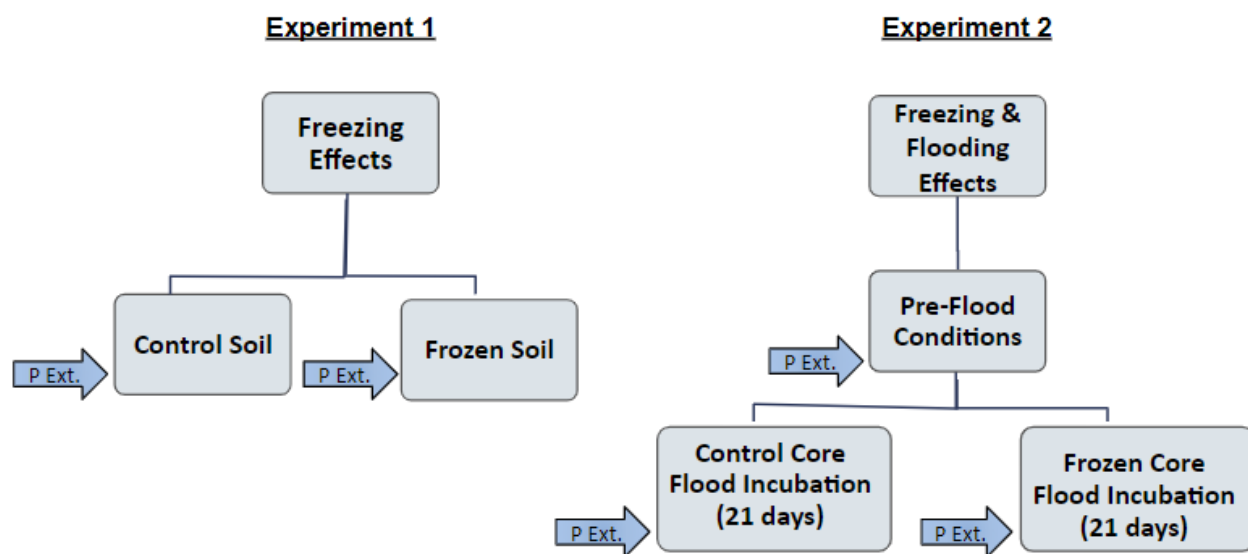


Figure 3 Experimental design scheme, where boxes represent samples and arrows represent a full P-extraction scheme conducted on soils (detailed extraction scheme in Appendix A).

Experiment 1 assessed the maximum potential effect of freezing on soil physicochemical characteristics. Multiple samples were collected and combined to create a composite sample at each of the 24 locations as described previously. Composite samples were taken back to the lab in plastic bags to maintain field moisture, homogenized, and split into 50 ml test tubes as control and frozen treatments. Frozen samples were stored in the freezer at -18°C for one week (days 1-7) before being thawed at 4°C for three days (days 8-10) and room temperature for several hours. Freezing and thawing temperatures were based on the equipment available. All analyses were conducted on field-moist samples within one week from the time of collection (unfrozen control, day 2) or following FT (day 10). Samples were refrigerated in between soil P and metal extractions. All soil samples were analyzed for moisture content, organic matter, carbonate, bulk density, carbon and nitrogen using split samples from homogenized composite samples. Phosphorus

extractions were performed on unfrozen control soils the week immediately after sampling (days 2-7); FT treatment soils were extracted after undergoing FT (days 11-15).

Sequential Phosphorus and Metal Extractions

A series of sequential extractions adapted from Pacini & Gächter (1999) and Darke & Walbridge (1994) based on the design of Noe et al. (2019) was performed following treatment to evaluate how the relative distribution of P into different soil fractions changes with freezing (Appendix A). A subsample of approximately 1g dry weight equivalent of soil was extracted sequentially using: 1) NH_4Cl to determine bioavailable P; 2) DCB (sodium dithionite, sodium citrate, and sodium bicarbonate) to measure redox sensitive soil P usually associated with iron oxides; 3) NaOH to measure less mobile Al bound soil P and P tied in organic, humic/microbial substances; and 4) HCl to measure carbonate P pools. Water extractable P was also determined on a separate 2g dry weight equivalent sample to measure labile P.

A second extraction scheme was used following treatment to isolate crystalline and non-crystalline aluminum and iron in soils as well as their associated P fractions (Darke & Walbridge, 1994). A dry weight equivalent of 0.4 g soil from each treatment was extracted using: 1) 40 mL of ammonium oxalate to isolate more reactive amorphous fractions of Al and Fe (Amox-Al and Amox-Fe); and 2) 40 mL NaOH to isolate crystalline, less reactive Al and Fe. A separate 0.8 g dry weight equivalent soil subsample was extracted using DCB (32 mL sodium citrate, 8 mL 1M sodium bicarbonate, & 0.8 g dithionite) to measure redox-sensitive amorphous and crystalline Al and Fe. To estimate crystalline Fe, Amox-Fe was subtracted from DCB-Fe (Appendix A- metal extraction scheme).

Soil samples were weighed into 50 ml centrifuge tubes for each set of extractions. Extraction solution was added to the tube, vortexed for 5s and shaken on a tube rotator at room temperature for a predetermined amount of time based on the method. After shaking, tubes were placed in a centrifuge for 10 minutes and filtered through 0.45-micron filters into centrifuge tubes. Filtered extractants were run for SRP via the molybdate blue color method (Murphy & Riley, 1962) on a discrete analyzer along with solution blanks for quality control. In addition to SRP, NaOH extractants were run for TP via alkaline persulfate digestion in an autoclave for 1 h (Patton, 2003).

NRP was calculated as the difference between TP and SRP (Appendix A). Metal extractants as well as the DCB-extracted P were run for total Fe, Al, Mn, and P via inductively coupled plasma-optical emission spectroscopy analysis.

1.3.4 Experiment 2: Phosphorus Release to Surface Water Following Flooding Compared to Flooding after Freeze-Thaw

Two soil cores were collected from each of the 6 floodplain locations at all 4 sites (n=48) to investigate the influence of soil properties on P release during flooding using experimental microcosm flood incubations and evaluate changes in the primary pools of P (Figure 3). Cores were collected in duplicate using 7.62 cm diameter PVC to a depth of 10 cm, vegetation was gently removed from the soil before sampling, cores were then capped and transported back to the lab in coolers. The duplicate cores were collected during the first week of January 2018 to ensure antecedent conditions would be like those experienced in-situ before freezing (Henry, 2007; Macrae et al., 2010). It should be noted that isolated soil frost may have existed prior to experimental freezing. Soil temperatures recorded at the Davis Purdue Agricultural Center, located approximately 140 km east of the sampling locations showed that bare soil temperatures at a depth of 10 cm reached daily minimum temperatures of 0°C twice during the week prior to sampling, but were at that temperature for less than a day, and minimum soil temperatures the week of sampling were consistently 1°C (DPAC, 2018). As in the first experiment, a separate subset of soil from each site was collected using a soil probe, homogenized, and used to measure initial soil physicochemical characteristics as well as soil P and metal chemistry pre-flooding.

Flood Microcosm Incubations

Potential P release following flooding with and without FT was evaluated using laboratory microcosm experiments. Duplicate cores were split into a control core flooded with site water the day after collection, and a core that was frozen at -18°C for one week before thawing and flooding. Frozen cores were thawed at 4°C for 3 days. All experiments were conducted at room temperature to maintain consistency and assess relative changes among sites and treatments. Site water for flooding was collected from the edge of the river at each of the four sites on the same day as core collection for the control cores. Water for incubation of the frozen cores was collected the day prior to experimental flooding and stored overnight at 4°C. Water chemistry measurements

including dissolved oxygen, pH, and turbidity were recorded at the start of experimental flooding. River water collected for frozen cores was lower in nutrients and colder at the time of collection compared to water collected for the control cores (Table 2).

Using rubber caps and rings, cores were made watertight and flooded with approximately 800 mL of respective site water. Organic debris that floated to the top of the water column after flooding was immediately removed. A blank core containing only site water was also established for each site. Flooded cores were placed in an enclosed water bath, temperature was recorded daily and adjusted to 20°C by adding ice or cool water. Sampling of overlying flood water took place at predetermined intervals of 0 h, 2 h, 8 h, 1 day, 2 days, 4 days, 8 days, 14 days, and 21 days, however core water was gently mixed once a day regardless of sampling. Using a 25 ml syringe with tubing attached, floodwater was gently mixed, and 5mL or 15 mL samples were collected 5 cm below the water surface. In addition, a multiparameter sonde was used after sample collection to measure the dissolved oxygen, pH, and temperature of overlying water in each of the cores throughout the incubation. Water samples were filtered through 0.45-micron filters and analyzed for ammonium (NH_4), nitrate (NO_3), and phosphate (PO_4) concentrations using standard EPA methods (EPA 103; EPA 114; EPA 118) on a discrete analyzer. Minimum detection limits (MDLs) were 0.002 mg NH_4L^{-1} , 0.03 mg NO_3L^{-1} and 0.004 mg PO_4L^{-1} respectively. Total dissolved N and total dissolved carbon were analyzed using the combustion catalytic oxidation method on a TOC-L (Potter & Wimsatt, 2005). Time 0 nutrient concentrations were subtracted out from each timepoint to calculate net change. Floodwater volume remaining in the core at the end of the incubation and sample volume removed at each time were used to calculate water volume at each timepoint. Core water volume was then multiplied by sample concentrations to calculate P release in mg.

Phosphorus and Metal Extractions

The same series of sequential extractions for P fractionation and metal content used in Experiment 1 (Appendix A- extraction scheme) was run on baseline pre-flood soils to evaluate conditions in soil on the day of collection. To evaluate changes in these pools with flooding, extractions were run on post-flood unfrozen control core soils. Soils from FT treatment cores were subjected to the same extraction scheme following flooding to evaluate changes with freezing and flooding.

Flooding effects were determined by comparing baseline pre-flooding soil characteristics to post-flooding unfrozen control treatment core soils. Additional changes with flooding influenced by FT were evaluated by comparing post-flood unfrozen control core soils to post-flood FT treated core soils (Figure 3).

1.3.5 Soil Physicochemical Characteristics

Composite soil samples from experiment 1 were analyzed for moisture, organic matter, carbonate, bulk density, carbon and nitrogen using the same homogenized samples collected for unfrozen control and FT treatment. Moisture content was measured gravimetrically upon returning to the lab as a percentage of the difference between field moist and dry soils after a constant dry weight was achieved in a drying oven at 60°C. The loss on ignition method was used to estimate organic matter and carbonate within each sample after burning at 550°C for 4 hours and 950°C for 2 hours respectively (Heiri et al., 2001). Bulk density was calculated using the dry weights of soil samples and the volume of the bulk density core. Dried, ground, and 2mm sieved soils were used to measure particle size via laser diffraction (Mastersizer 3000, Malvern Instruments, Worcestershire, UK) following dispersion with sodium hexametaphosphate and total soil carbon and nitrogen via combustion (Wright & Bailey, 2001). Soil classifications were determined using the USDA Natural Resources Conservation Service web soil survey tool (Soil Survey Staff, 2019).

Composite soil samples collected as pre-flood baseline samples for experiment 2 were analyzed for moisture, organic matter, carbonate, bulk density, particle size, carbon and nitrogen using the same methods described for Experiment 1. Gravimetric moisture content and organic matter were the only physicochemical properties measured from post-flood core soils in both unfrozen control and FT treatments.

1.3.6 Statistical Analyses

Total extractable P (TEP) and total extractable Fe and Al were calculated as the sum of all extractable P and metal pools from the sequential extractions expressed in mg/g dry weight equivalent of soil. P release was calculated as a net release in mg based on starting nutrient concentrations of floodwater and remaining water volume in each core at the end of the incubation.

Statistics were run using R 3.5.0 (R Core team, 2018), the dplyr (Hadley et al., 2018), leaps (Lumley, 2020), olsrr (Hebbali, 2020), and pwr (Champely, 2020) packages. For all statistical analyses, significance was set at $\alpha = .05$.

1.3.7 Experiment 1: Potential Impact of Freezing and Thawing on Soil Extractable Metals & Phosphorus

Experiment 1 soil samples were analyzed to look at the potential changes in metals and P pools following a single freeze-thaw event. Paired t-tests were used to evaluate statistical differences between the control and frozen treatments, paired by sampling location, for each experimental pool. Phosphorus pools were expressed as a proportion of TEP at that location for statistical analyses under the assumption it would minimize minor sample differences that may exist even in homogenized composite samples. Differences between treatments were checked for normality using the Shapiro-Wilk test. Effect sizes for paired t-tests were calculated as Cohen's d for t-tests:

$$d = \frac{mean_D}{SD_D}$$

Where D is the difference in the paired sample values and considered small ≥ 0.20 , medium ≥ 0.50 , and large ≥ 0.80 (Cohen, 1988).

1.3.7.1 Experiment 2: Changes in Phosphorus Release During Flooding After FT

Differences in P released during flooding alone versus P released during flooding after FT were evaluated using Wilcoxon signed-rank tests for paired samples. To identify how treatment effects changed with inundation time, signed-rank tests were run for P release across all sampling times as well as for P release at each individual timepoint. Assumptions and effect sizes were calculated as described in Experiment 1.

Drivers of Phosphorus Release at Important Timepoints (4 days, 8 days, 14 days)

Because treatment effects varied at different inundation times, the factors influencing P release at three timepoints (4, 8, and 14 days) associated with the greatest treatment differences in P release were assessed. The all-subsets regression method was used to produce the best multiple linear

regression model for P release. All-subsets regression uses three model statistics to determine the best subset of variables to include in the multiple linear regression model (Helsel et al., 2020). These model statistics include Mallows's C_p , which is designed to find compromise between explaining variance by including more variables and minimizing standard error by keeping the coefficients small; the Bayesian information criterion (BIC), which also aims to increase the goodness of fit while keeping the number of explanatory variables small; the adjusted R^2 (R_a^2), which aims to account for the loss in the degrees of freedom associated with additional variables that increase R^2 . Variables included in the all-subsets regression were chosen based on exploratory analyses of the data including correlation matrices and PCAs in addition to the literature on P release in floodplains: organic matter; calcium carbonate (CaCO_3); % Clay; % Sand; Amox- P; Amox-P: NaOH- P; Amox P: Amox Al + Fe; Amox Fe; Crystalline Fe; Total extractable Al; Total extractable Fe; NaOH-SRP; NaOH-NRP; DCB- SRP; HCl-SRP; TEP; and water column temperature, pH, dissolved oxygen (DO), NO_3^- , NH_4^+ , dissolved organic carbon (DOC), and dissolved organic nitrogen (DON) measured at the time of sampling.

Final models were selected after evaluating the models selected in the all-subsets regression analysis based on the model statistic C_p as it consistently produced the simplest models with similar predictive power to the adjusted R^2 and BIC. The C_p statistic is calculated as:

$$C_p = p + \frac{(n - p)(MSE_p - \hat{\sigma}^2)}{\hat{\sigma}^2}$$

Where n is the number of observations, p is the number of coefficients, MSE_p is the mean square error of the p -coefficient model and is the estimate of the true error, which is inferred to be the minimum MSE (Helsel et al., 2020). Low C_p values correspond with the most parsimonious model.

Model residuals were checked for normality using Q-Q plots and transformed as needed. 14-day P release models for both treatments met the assumptions of linearity, normality and homoscedasticity, while the 8-day control treatment and 4 day FT treatment P release models required transformations to meet the model assumptions. A square root transformation was used on P release in the 4-day and 8-day models to meet the assumptions; all-subsets regression was rerun after the transformation and assumptions for the new models rechecked. Standardized coefficients for model variables were calculated as Beta (β) where:

$$\beta = \frac{\text{Coefficient} \times SDx}{SDy}$$

Sequential Extraction Phosphorus Pools and Metals

To evaluate potential treatment effects of flooding alone on extractable metals and P within soil, Wilcoxon signed rank tests were run on composite soil samples analyzed pre-flood incubation (experiment 1) and soil samples taken from the unfrozen control core post-incubation (experiment 2) (Figure 3) (Helsel et al. 2020). Nonparametric tests were used because data were not normally distributed and sample sizes were small. To evaluate changes with freezing and flooding, soil samples taken from experiment 2 unfrozen control and frozen cores post-flooding were compared (Figure 3). Effect sizes were calculated by dividing the absolute standardized test statistic Z by the square root of the number of pairs (24) for signed-rank tests.

1.4 Results

1.4.1 Experiment 1: Potential Impact of Freezing and Thawing on Soil Extractable Metals & Phosphorus

Freezing Effects on Extractable Phosphorus

Total extractable P (TEP) is the sum of all sequentially extracted P pools in mg g⁻¹ dry weight equivalent (Dweq) of soil. Total Extractable P was not significantly different (Figure 4), in frozen compared to unfrozen soil samples (M=0.752 mg g⁻¹ and M=0.672 mg g⁻¹ in unfrozen and frozen samples respectively, pairwise t-test; p=0.105). Freezing did have a significant impact on the relative proportion of several P pools, however (Figure 4). NaOH-extractable SRP in FT samples accounted for a moderately smaller proportion of TEP when compared to unfrozen control samples (M=0.08 and M=0.13 for FT and unfrozen samples respectively, p=0.006). Inversely, unfrozen control samples had a slightly smaller proportion of DCB-extractable SRP than FT treated samples (M=0.574 and M=0.652; p=0.028). All other changes in extractable P pools were not significantly different after one FT cycle. Additional data on the concentrations of extractable P in soils can be found in Appendix B (Table 1).

Freezing Effects on Extractable Metals

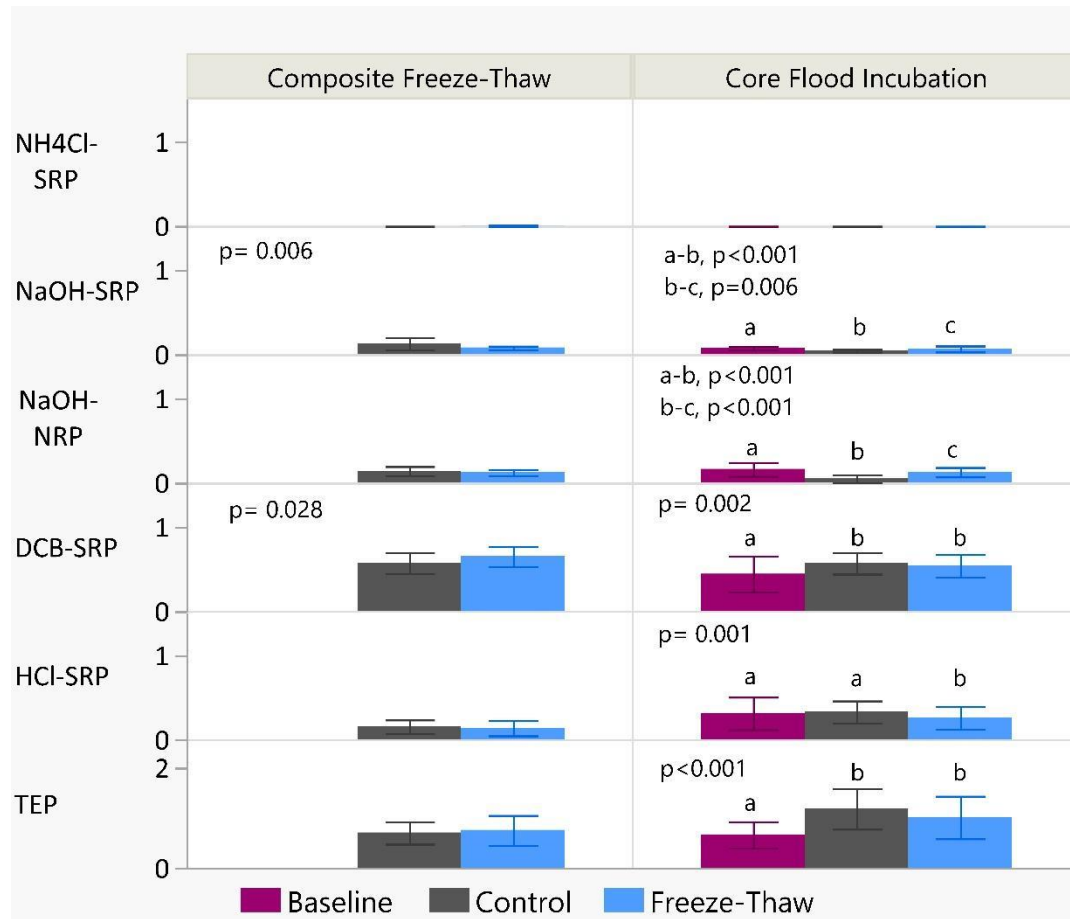


Figure 4- Total extractable P (TEP) in mg g⁻¹ Dweq soil from sequential P extractions and the mean proportion of each pool within TEP. Bars represent one standard deviation (SD). Letters represent significant differences between treatments.

Nonparametric tests revealed that FT of composite samples led to decreases in almost all extractable metals and associated P (Figure 5). Ammonium oxalate extractable amorphous metals were slightly smaller post freeze-thaw except for Mn which was not significantly different. NaOH extractable crystalline metals behaved similarly, with small decreases following FT. Phosphorus bound to crystalline metals was impacted by freezing (Mdn=0.102 mg g⁻¹ unfrozen soil; Mdn=0.032 mg g⁻¹ FT soil; Wilcoxon signed-rank test; $p < 0.001$) to a larger degree than P bound to amorphous metals post FT (Mdn=0.395 mg g⁻¹ unfrozen soil; Mdn=0.336 mg g⁻¹ FT soil; $p = 0.04$). Additional data on extractable metals can be found in Appendix B1 (Table 1).

1.4.2 Experiment 2: Phosphorus Release to Surface Water Following Flooding Compared to Flooding after Freeze-Thaw

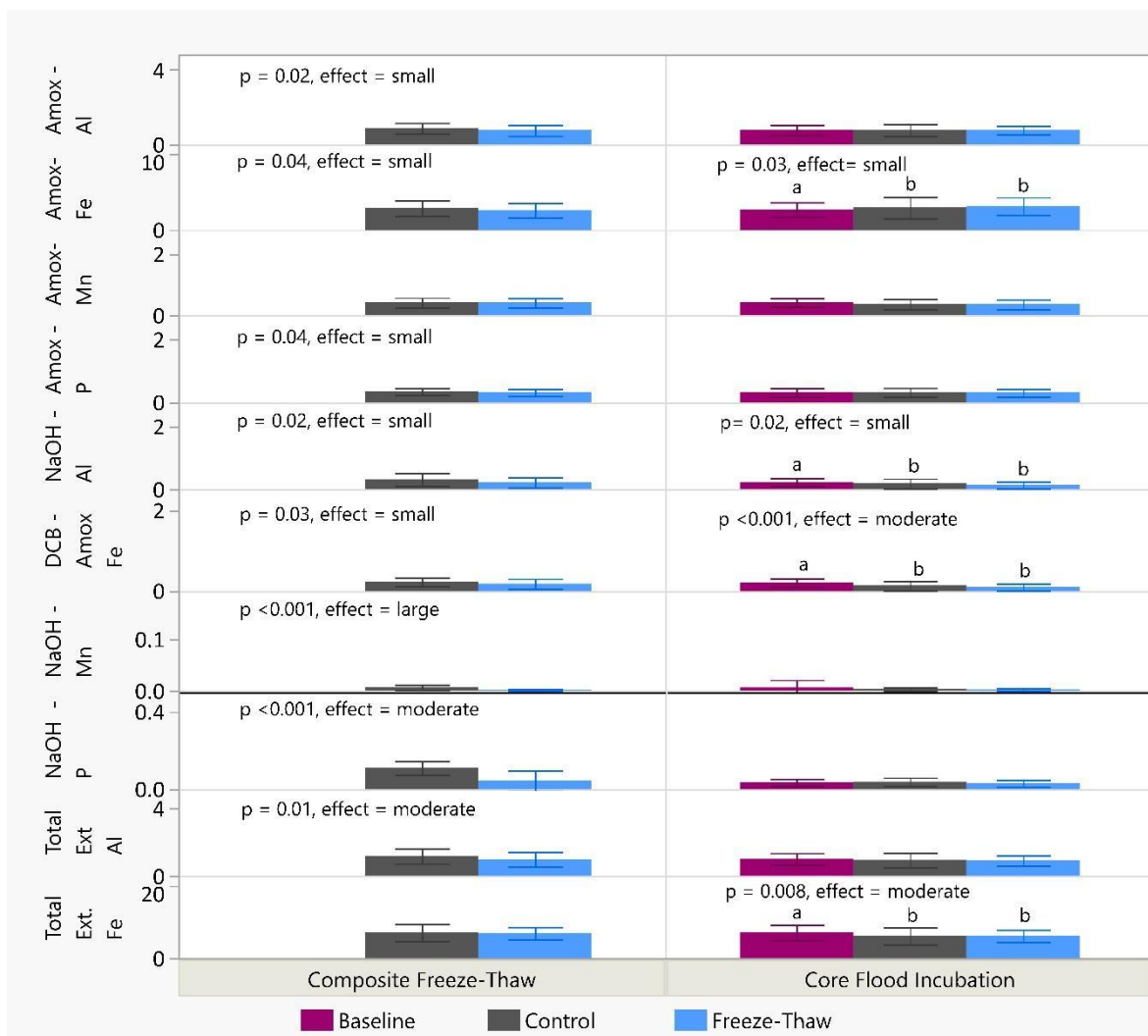


Figure 5- Mean extractable metals reported in mg/g Dweq soil. Bars represent 1 standard deviation. Letters indicate significant differences between samples as indicated by p-values of Wilcoxon signed-rank tests run on paired samples.

Flooding and FT Effects on Extractable Phosphorus

Unfrozen control soils had higher TEP after flooding compared to pre-flooded soils (hereafter termed “baseline”) (Figure 4) ($M=1.18 \text{ mg g}^{-1}$ and $M=0.661 \text{ mg g}^{-1}$ respectively, paired t-test; $p < 0.001$). This higher TEP was accompanied by changes in the distribution of the pools of P within the soil. Unfrozen control soils at the end of the flooding experiment had higher proportions of

DCB extractable SRP than pre-flooding baseline soils ($M=0.57$ & $M=0.44$ respectively; $p=0.002$). At the same time, NaOH extractable SRP ($M=0.05$ mg g^{-1} and $M=0.08$ mg g^{-1} for post-flood and baseline soils respectively, $p<0.001$) and NRP ($M=0.05$ mg g^{-1} and $M=0.16$ mg g^{-1} for post-flooding and baseline soils respectively, $p<0.001$) in unfrozen control soils after flooding accounted for a much smaller proportion of TEP compared to baseline. HCl extractable P was not significantly different after flooding.

Flooding following FT led to small reductions in soil TEP compared to unfrozen cores post-flooding (Figure 4) ($M=1.01$ mg P g^{-1} FT treatment soil and $M=1.18$ mg P g^{-1} unfrozen control soil respectively, paired t-test, $p=0.04$). Ratios of extractable P pools were also impacted by the FT treatment, except for DCB-extractable P which showed no significant change. The largest difference was seen in the NaOH extractable NRP proportion, which was twice as high on average in FT treatment cores than in unfrozen control cores ($M=0.13$ and $M=0.05$ respectively, $p<0.001$). NaOH extractable SRP was moderately higher in FT treatment cores compared to unfrozen control cores as well ($M=0.07$ and $M=0.05$ respectively, $p=0.006$). HCl extractable P was the only proportion of P to decrease after flooding with FT compared to unfrozen cores ($M=0.26$ and $M=0.33$ respectively, $p=0.001$).

Flooding and FT Effects on Metals

The 21-day simulated flooding conditions generally decreased soil extractable metals (Figure 5). Decreases were seen in crystalline NaOH-extractable Al and Fe following flooding (Al $\text{Mdn}=0.207$ mg g^{-1} and $\text{Mdn}=0.15$ mg g^{-1} for unfrozen flooded cores and FT flooded cores respectively; Wilcoxon signed-rank test; $p=0.02$) (Fe $\text{Mdn}=0.177$ mg g^{-1} and $\text{Mdn}=0.09$ mg g^{-1} for unfrozen flooded cores and FT flooded cores respectively, $p<0.001$). Amorphous ammonium oxalate extractable Mn also showed significant decreases following flooding ($\text{Mdn}=0.439$ mg g^{-1} and $\text{Mdn}=0.374$ mg g^{-1} respectively, $p=0.04$). All other metal pools were not significantly different. Amorphous and crystalline metal bound P were also not significantly different after flooding. Wilcoxon signed-rank test run on core soil properties post flooding paired with flooding after FT revealed no significant differences in extractable metals or associated P pools.

Freezing and Thawing Treatment Effect on P Release

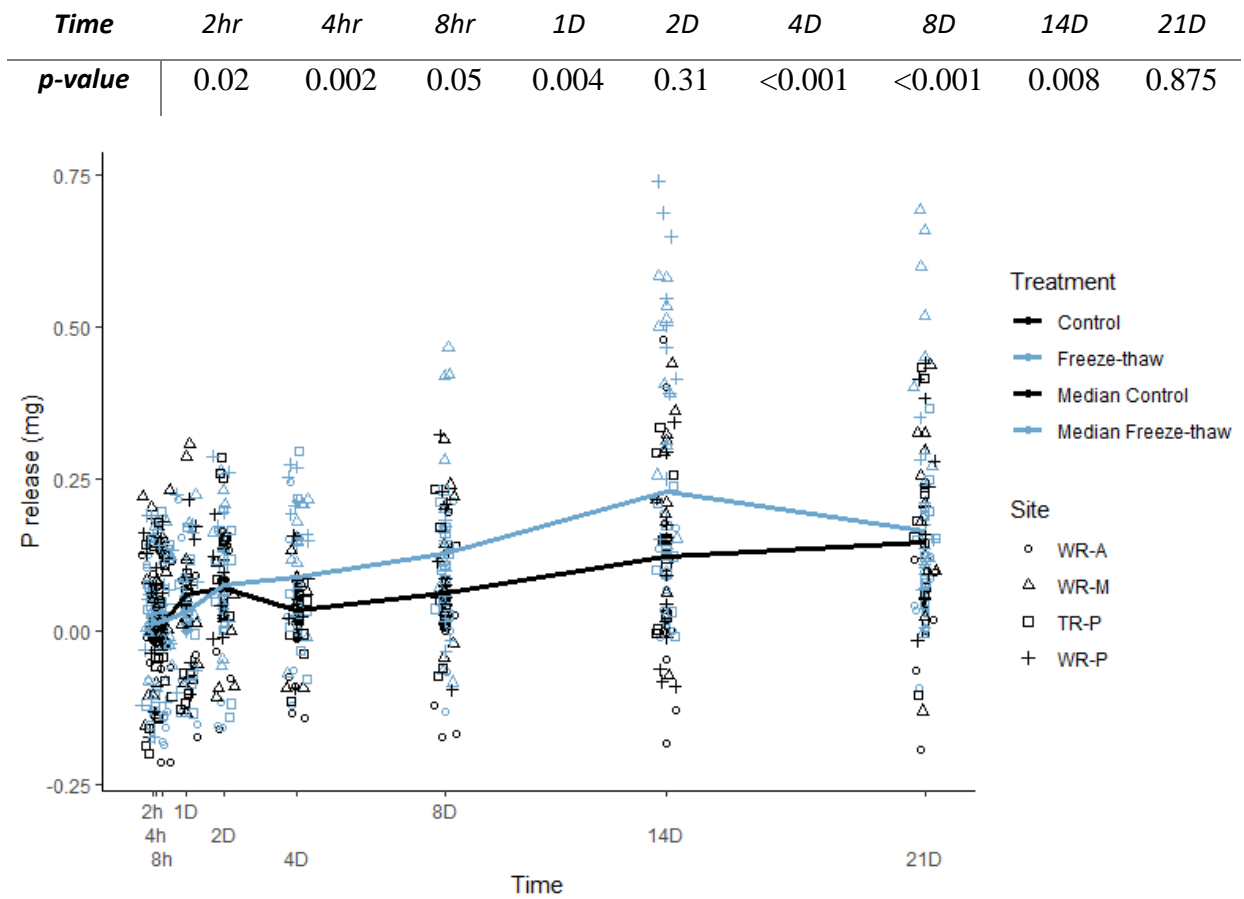


Figure 6 Median SRP (mg) released in control and treatment cores by each sampling timepoint. Points represent individual cores. P-values obtained from Wilcoxon signed-rank tests.

Phosphorus released to overlying surface water during flooding was impacted by the FT treatment (Figure 6). P release was calculated using the starting water nutrient concentrations before flooding (Table 1). Wilcoxon signed-rank tests for each sampling period revealed that FT treatment effects were stronger at certain timepoints during the incubation. In the first 2 hours of flooding, unfrozen control cores released less P than FT treatment cores (Mdn=0.003 mg and Mdn=0.01 mg respectively; Wilcoxon signed-rank test; $p=0.02$). Phosphorus concentrations in the water column of the unfrozen control cores decreased from 2 to 4 hours while FT treatment cores remain at similar levels (Mdn=-0.01 mg and Mdn=0.01 mg respectively, $p=0.002$). This trend continued until day 1 when P release in the unfrozen control cores exceeded P release in the FT treatment cores (Mdn=0.042 mg and Mdn=0.02 mg respectively, $p=0.004$). At 2 days of flooding both cores released similar amounts of P. After 2 days, FT treatment cores continuously released more P to

the water column than unfrozen control cores until reaching their maximum release at 14 days. Unfrozen control cores after 4 days of flooding released less P compared to FT treatment cores (Mdn=0.032 mg and Mdn=0.063 mg respectively; $p<0.001$). Similar effects were seen in FT treatment cores at 8 days (Mdn=0.113 mg and Mdn=0.052 mg for FT treatment and unfrozen control cores respectively, $p<0.001$). While the effect of FT treatment was slightly smaller at 14 days, this appeared to be the maximum P released throughout the incubation in the FT treatment cores (Mdn=0.138 mg and Mdn=0.112 mg for FT treatment and unfrozen control cores respectively, $p=0.001$).

Table 1 Starting water chemistry for flood incubations where nutrient measurements were taken before flooding and temperature, dissolved oxygen, and pH were measured 2 hours after the onset of flooding.

Control Cores

Time 0 / 2hr

Site	WR-A	WR-M	TR-P	WR-P	Average
Temp -2hr (°C)	17.94	17.75	17.47	17.05	17.55
DO -2hr (mg L⁻¹)	12.53	12.42	12.64	12.25	12.46
pH -2hr	8.23	8.31	8.30	8.24	8.27
PO₄ (mg L⁻¹)	0.03	0.00	0.01	0.02	0.01
NO₃ (mg L⁻¹)	5.81	6.37	6.14	5.20	5.86
NH₄ (mg L⁻¹)	0.11	<MDL	<MDL	<MDL	<MDL

Frozen Cores

Time 0 / 2hr

Site	WR-A	WR-M	TR-P	WR-P	Average
Temp -2hr (°C)	13.88	18.77	12.67	18.85	15.79
DO -2hr (mg L⁻¹)	12.55	11.66	12.91	11.49	12.14
pH -2hr	8.34	8.29	8.33	8.32	8.32
PO₄ (mg L⁻¹)	<MDL	<MDL	<MDL	<MDL	<MDL
NO₃ (mg L⁻¹)	1.81	1.21	0.49	4.82	1.51
NH₄ (mg L⁻¹)	<MDL	<MDL	<MDL	<MDL	<MDL

Drivers of Phosphorus Release

Four days after the onset of flooding, P release in control cores was predictable using a combination of soil characteristics (Table 2) (square root transformation, $R^2 = 0.78$, $p<0.001$): Amox- Al ($\beta = -0.59$), DCB-SRP ($\beta = 0.40$), and Amox- Fe ($\beta = 0.33$) and water column DOC ($\beta =$

0.99) and DON ($\beta = 0.89$). Regression models for P release (square root transformed) after 4 days in FT treatment cores also were highly predictable using a combination of soil characteristics and overlying water chemistry ($R^2 = 0.91$, $p < 0.001$): Amox-Al ($\beta = 2.49$), total extractable Al ($\beta = -1.73$), TEP ($\beta = 0.87$), the ratio of amorphous metal bound P to crystalline metal bound P ($\beta = -0.56$), total extractable Fe ($\beta = -0.49$), and HCl-extractable SRP ($\beta = -0.42$), as well as water column NO_3 ($\beta = -0.94$) and DON ($\beta = 0.54$).

Table 2- Mean physicochemical properties by site measured pre-flooding. Where, BD= bulk density; OM=organic matter; MC= moisture content; TEP= Total Extractable P; T. Ext= total extractable; WR-A = Wabash R. Agriculture; WR-M = Wabash R. Mitigation; TR-P

	WR-A	WR-M	TR-P	WR-P
Soil type	Silt loam & Sandy loam	Silt loam	Silty clay loam & silt loam	Silt loam
BD g cm^{-3}	1.6 (± 0.16)	1.2 (± 0.25)	1.3 (± 0.13)	1.3 (± 0.03)
C g kg^{-1}	14.6 (± 0.72)	43.3 (± 0.28)	34.9 (± 1.09)	37.6 (± 1.89)
N g kg^{-1}	0.6 (± 0.07)	2.4 (± 0.03)	2.4 (± 0.06)	2.1 (± 0.05)
OM %	3.1 (± 1.91)	6.9 (± 1.82)	6.8 (± 1.84)	6.6 (± 0.37)
MC %	17.3 (± 3.77)	29.5 (± 4.78)	27.7 (± 5.11)	26.1 (± 1.15)
CaCO_3 %	2.0 (± 0.49)	6.2 (± 0.33)	3.0 (± 2.21)	5.7 (± 0.29)
Clay %	8.4 (± 6.79)	10.9 (± 2.14)	10.5 (± 4.42)	10.3 (± 3.39)
Silt %	47.8 (± 0.15)	68.5 (± 2.59)	66.4 (± 8.14)	69.7 (± 1.90)
Sand %	34.7 (± 0.21)	20.0 (± 4.24)	19.9 (± 11.6)	19.2 (± 4.03)
TEP mg g^{-1}	0.3 (± 0.15)	0.7 (± 0.19)	0.9 (± 0.19)	0.7 (± 0.17)
T. Ext Al mg g^{-1}	0.5 (± 0.32)	0.9 (± 0.13)	1.3 (± 0.23)	1.1 (± 0.11)
T. Ext Fe mg g^{-1}	4.2 (± 2.91)	8.0 (± 0.48)	7.8 (± 1.65)	7.5 (± 0.98)

P release in unfrozen control cores after 8 days of flooding was predicted using mostly soil characteristics (square root transformed, $R^2 = 0.88$, $p < 0.001$): amorphous P:crystalline P ($\beta = 1.13$), TEP ($\beta = 0.80$), total extractable Al ($\beta = -0.71$), HCl-extractable SRP ($\beta = -0.58$), amorphous P:amorphous Fe + Al ($\beta = -0.56$), and clay ($\beta = -0.55$); NO_3 was the only water chemistry variable included ($\beta = -0.46$). P release in FT treatment cores after 8 days was also highly predictable ($R^2 = 0.97$, $p < 0.001$) by a combination of soil Amox- P : Amox-Al +Fe ($\beta = -0.81$), NaOH-NRP ($\beta = -$

0.71), Amox- P : NaOH- P ($\beta = 0.44$), sand ($\beta = -0.39$), HCl-SRP ($\beta = 0.39$), total-extractable Fe ($\beta = 0.35$), and water column pH ($\beta = -0.79$) and NO_3 ($\beta = 0.62$).

For P release models 14 days into flooding, several variables were included in control core regression models to achieve the high predictive power ($R^2 = 0.92$, $p < 0.001$): DCB-extractable SRP ($\beta = 8.77$), NaOH-NRP ($\beta = 2.44$), HCl-extractable SRP ($\beta = 1.8$), TEP ($\beta = -1.18$), sand ($\beta = -0.69$), Amox-Al ($\beta = -0.54$), and Amox-P: Amox-Fe + Al ($\beta = 0.42$). Water column variables included were pH ($\beta = -1.7$), DO ($\beta = 1.69$), DOC ($\beta = -0.83$), NO_3 ($\beta = -0.72$), and temperature ($\beta = 0.42$). The regression model for P release in FT treatment cores at 14 days, the maximum release point during the flood incubation, was largely predictable using soil characteristics ($R^2 = 0.91$, $p < 0.001$): NaOH-NRP ($\beta = -1.13$), Amox-Al ($\beta = 0.62$), total extractable Fe ($\beta = 0.37$) HCl-SRP ($\beta = 0.33$), Amox- P : Amox- Al+ Fe ratio ($\beta = -0.3$), and sand ($\beta = -0.275$); DOC ($\beta = 0.47$) was the only included water chemistry variable.

1.5 Discussion

1.5.1 Experiment 1: Potential Impact of Freezing and Thawing on Soil Extractable Metals & Phosphorus

Freezing Effects on Extractable Phosphorus

Labile P, measured by NH_4Cl extraction, was negligible in most samples across all treatments, supporting the idea that P released into porewater is cycled quickly into other soil pools. This was somewhat surprising as other floodplain restoration studies have found that labile reactive P can be a predictor of P release during flooding (Noe et al., 2019). This also contrasts from findings on disturbance regimes like drying rewetting which showed that labile P (measured as water extractable P) was a strong predictor of P release following re-wetting of dried wetland soils (Smith & Jacinthe, 2014).

The NaOH-SRP pool decreased and the DCB-SRP pool significantly increased following FT (Figure 4). A possible mechanism to explain this trend is that P released from clay during freezing was quickly adsorbed onto ferric soil surfaces. The NaOH-SRP pool is generally attributed to clay bound-P, inorganic P compounds, or Al-oxide exchangeable P, while the DCB-SRP pool is redox

sensitive and largely associated with P adsorbed onto Fe and Mn coated soil surfaces. Shearing during freezing may have broken up aggregates (Zhang et al., 2016), causing P bound to clay particles (i.e., NaOH-SRP) to become more exposed in the soil where it could then quickly be reabsorbed onto redox sensitive surfaces thereby effectively transferring a portion of the NaOH-SRP pool to the DCB-SRP pool. This contrasts with the hypothesis that P would be released from microbial lysis of cells during freezing, which would be supported by an increase in the labile NH_4Cl extractable pool.

Changes in extractable phosphorus pools in this study following a single FT cycle suggest that while FT may not impact total extractable P in floodplain soils, it likely redistributes P from one pool to another, in this case clay-bound (NaOH-extractable SRP) to more redox-sensitive pools (DCB-extractable SRP). Similarly, changes in extractable P pools following freezing were observed in a study by Sun et al. (2019), where freezing increased levels of both sodium bicarbonate extractable inorganic and organic P representative of the enzymatically hydrolysable P pool. The largest effects were observed following 2 FT cycles and diminished after, leading to the conclusion that differences in soil P were due to microbial cell lysis and aggregate disruption. However, in another study looking at P transformations in Chinese forest and grassland soils, no significant differences were found in total extractable P or P fractions after FT treatment of soils (Xu et al., 2011), suggesting setting and soil type may influence FT impacts. However, differences in extraction schemes also make it difficult to quantitatively compare P pools in soil across studies. Further, the impact of freezing in our experiment may be exasperated by the fact that soils were exposed to cold temperatures from all sides in the laboratory, which would not happen under field conditions.

Freezing Effects on Extractable Metals

Freezing consistently decreased extractable metal pools by small but significant amounts (Figure 5). Aggregated particles could have physically protected metals further, decreasing the extractable portion. However, changes in the soil structure post-freeze leading to the formation of larger aggregates are usually associated with more than one FT cycle over longer periods (Zhang et al., 2016; Mohanty et al., 2014; Blackwell et al., 2010), so it is unclear what is driving these patterns.

1.5.2 Experiment 2: Phosphorus Release to Surface Water Following Flooding Compared to Flooding after Freeze-Thaw

Flooding and FT Effects on Extractable Phosphorus

Soil TEP was significantly higher in control cores after flooding than in pre-flood baseline soils, suggesting or, more likely, that floodwater contributed new P to the soil system as starting floodwater concentrations were $0.01 \text{ mg L}^{-1} \text{ PO}_4$ on average. While there was no significant difference in soil TEP between FT and control cores post-flooding, the relative proportions of extractable P did show some changes indicating dynamic P cycling in response to freezing and to flooding. The largest effects of flooding were reductions in the NaOH-extractable SRP pool and the NaOH-extractable NRP pool between pre-flood soils and post-flood control soils. Others have also documented significant reductions in the NaOH extractable inorganic P pools with flooding (SurrIDGE et al., 2007); however, FT treatment soils had significantly more of these pools post-flooding than the control treatment soils. This indicates that flooding may have led to the dissolution of P from clay particles or desorption from aluminum oxides as NaOH-SRP is generally attributed clay bound-P, inorganic P compounds, or Al-oxide exchangeable P (Pacini & Gatcher, 1999). The greater NaOH-SRP in frozen than control cores after flooding was similar to the effects of freezing alone (see prior section). Further, the patterns suggest that NaOH-NRP may have been broken down by microbes in control cores during the incubation, but not in FT treatment core soils. This is supported by the observed NaOH-NRP that was twice as high on average in FT treatment soils (Figure 4). Alternatively, microbial lysis during freezing may have contributed to the higher NaOH-NRP which can be associated with detritus organic-P and other refractory organic P fractions.

The HCl-extractable pool, which represents Ca associated P, was not significantly different post-flooding than pre-flooding. HCl-extractable P was significantly less in the post-flooding FT cores than the control cores, however. This suggests that dissolution of Ca-phosphates from the soil to the overlying water was enhanced by freezing before flooding. In a study by Kumaragamage et al. (2020) looking at the influence of floodwater temperature on P released following flooding in moderately calcareous soils, they found increases in porewater Ca for the first 7 days after flooding and decreases with additional days under cold flooding conditions, which is in agreement with our

finding that CaCO_3 in soils had a strong effect through day 8 of flooding in FT treatment cores. They also saw increasing Ca and Mg concentrations in floodwater with days after flooding that they correlated strongly with floodwater DRP under warm flooding conditions, suggesting that dissolution played a significant role in P released to floodwater (Kumaragamage et al., 2020).

Flooding and FT Effects on Extractable Metals

Freezing consistently decreased extractable metal pools by small but significant amounts as described previously. After flooding, crystalline (NaOH-extractable) Al decreased, suggesting flooding may alter the ratio of amorphous: crystalline P and in turn the P released to the water column. This is similar to findings in forested floodplain soils (Darke & Walbridge, 2000). Higher amorphous: crystalline ratios have been associated with greater P sorption in studies investigating the increased crystallinity of iron hydroxides with drying (Schönbrunner et al., 2012; Darke & Walbridge, 1994). For this reason, the ratio of amorphous: crystalline metal associated P was included as a model variable in P release analysis. However, others have found no significant changes in Al or Fe with flooding in slightly acidic sandy loam floodplain soils (Wright et al., 2001), highlighting the need for this research in a variety of soil types.

Freezing and Thawing Effect on Phosphorus Release

Flooding after FT showed significant differences in P released during the 21-day flood incubation compared to flooding of unfrozen soils. Control cores appeared to have more complex P cycling dynamics as water column P fluctuated throughout the duration of the flood incubation, suggesting some internal cycling and release was occurring. Freeze-thaw treatment cores consistently released P until the very end of the incubation when concentrations decreased in the water column. The consistent positive flux of P from the soil to the water column could be explained by microbial die-off in the treatment cores caused by freezing thereby slowing reassimilation of P by the microbial community (Blackwell et al., 2010). Conversely, microbes remaining in the soil in the unfrozen control cores were able to assimilate P from the water column during the initial few hours of flooding, during which time new pools of P were being released to the water column. Measurements of the microbial P pool were unavailable and would have helped to further define this mechanism. Additionally, inundated cores do not represent field dynamics of flooding in that

the water is stagnant with no vertical advection between soil and water column with only slight mixing before sampling. In fact, a study by Noe et al. (2019) found that P released in cores during lab flooding experiments was not representative of the magnitude of P released under field conditions, although relative differences among sites showed consistent patterns supporting this use of this method as a comparative tool. Other studies on long-term restored floodplains in England also found that P release measured in-situ exceeded that measured ex-situ (Surrice et al., 2012), however P ex-situ showed similar variability in the magnitude of P released in-situ in this study as well. This study therefore may not provide an absolute measure of P released at the floodplain sites, but it will measure relative differences and drivers of variability in P release following FT and flooding of floodplain soils, which is not well understood.

Drivers of Phosphorus Release

4 days

Four days after the onset of flooding in unfrozen cores, a combination of soil characteristics and overlying water column chemistry were able to reliably predict P release from soil to floodwater. Floodwater concentrations of P in unfrozen cores decreased between 2-days and 4-days of flooding and began to increase steadily after that (Figure 5). Soil characteristics like amox-extractable Fe and DCB-extractable SRP showed positive relationships with P released, while amox-extractable Al showed an inverse relationship. The influence of redox-sensitive Fe-P pools in soil on P release during flooding is well documented (Surrice et al., 2012; Noe et al., 2019; Gu et al., 2019; Christian et al., 2009; Darke & Walbridge, 2000). Studies have shown that biological processes can play a major role (Wright et al., 2001), but P in soils is often controlled by sorption-desorption processes with Fe or Ca depending on the soil system (Shenker et al., 2005; Jayarathne et al., 2016; Satchithanatham et al., 2019). The importance of extractable metals and metal-bound P pools in regression models provides evidence that redox conditions are influencing P release within the first 4 days of flooding. Phosphorus could have been released from amorphous Fe binding sites early in the incubation as indicated by the positive effect of Amox-Fe on P release, while simultaneously being bound onto amorphous Al (amox-extractable), or other sequentially extracted P pools (TEP) as indicated by their inverse relationship with P release. Aluminum is less affected by redox status compared to Fe and is a better predictor of P retention (Darke &

Walbridge, 2000), partially because Fe is used by microbes as an electron acceptor in the absence of oxygen (Hoffmann et al., 2009; Reddy et al., 2000). Although DO was not included in the model, we see an initial drop in DO levels within the first 4 days further supporting the influence of redox status on P dynamics.

Higher water column DON and DOC concentrations were associated with greater P release in control core regression models. This could be reflective of less microbial activity in cores with greater P release due to microbial death during early stages of flooding and/or release of nutrients from other forms of organic matter including plant residue. P was initially released to the water column as evidenced by increasing and highly variable concentrations during the first 2 days of flooding. P from the soil can be incorporated into microbial biomass along with other nutrients like C and N, decreasing water concentrations of dissolved nutrients. Denitrification, the microbial process responsible for NO_3 removal, occurs under anaerobic conditions. Consistent reductions in water column NO_3 until 8 days when concentrations started to level off further support the possible influence of microbes on P release from redox sensitive pools. Measured water column concentrations of P then showed a general decrease between 2 and 4 days after the start of flooding, which may have been due to binding with amorphous Al (Amox-extractable) or microbial uptake of P released from redox sensitive iron pools or a combination of the two.

Flooding after a freeze-thaw treatment produced different predictor variables of P release 4 days into flooding. Contrasting from the unfrozen control cores, P was steadily released between 2 and 4 days of inundation in the FT treatment cores (Figure 5). To explain P release, the FT treatment model included more variables than unfrozen control models and was able to make slightly better predictions. Soil characteristics included in the model showed both negative (Amox-P: NaOH-P, HCl-SRP, total Al and Fe) and positive (Amox-Al and TEP) effects on P release. The positive relationship between Amox-Al and P release is interesting this early in the incubation as amorphous Al is often associated with P sorption capacity (Darke & Walbridge, 2000; Noe et al., 2019), as we saw in the unfrozen control cores. However, the ratio of Amox-P to NaOH-P is negatively correlated, implying the relationship between amorphous Al and P bound in that pool is not always direct. The inverse relationship between amorphous: crystalline ratios of P and P availability is consistent with findings in other soils (Schönbrunner et al., 2012; Darke & Walbridge, 1994). Water DON, taken at the same time as P measurements, was positively

correlated to P release similar to the control cores, while NO_3 showed a negative relationship. This suggests lower concentrations of water NO_3 were associated with greater P release, and again may be indicative of microbial processes occurring in individual cores as denitrification happens under anaerobic conditions and removes NO_3 .

Differences in P release models between unfrozen treatment cores and FT treatment cores suggest that dynamics controlling P release differed based on treatment after 4 days of flooding. Phosphorus release in unfrozen control cores was controlled largely by redox sensitive Fe and Fe-associated P and influenced by overlying water chemistry (DOC, DON), while P retention was associated with amorphous Al (Amox-extractable); the opposite was observed in FT treatment cores. While FT treatment cores had P release that also appeared to be influenced by overlying water chemistry (DON, NO_3), amorphous Al and TEP in soils prior to flooding appeared to have a greater influence on P release. Retention in FT cores was associated with higher total extractable metals, Ca-P (HCl-extractable), and the ratio of amorphous (Amox-extractable) Al + Fe bound P to crystalline (NaOH-extractable) Al + Fe bound P in soils prior to flooding. The Ca-P (HCl-extractable) pool consistently emerged as a predictor variable of P release in FT treatment cores and was also reduced in soils following flooding compared to those that had not undergone FT, highlighting the importance of Ca-P as a control on P release in FT cores but not unfrozen cores.

8 days

Water column P increased between 4 and 8 days of flooding and continued to increase in both unfrozen flooded cores and FT flooded cores (Figure 5). Predictor variables of P release after 8 days of flooding in unfrozen flooded cores changed compared to 4-day models and the predictive power increased. The soil conditions pre-flooding were more important than water chemistry at this timepoint, as only water column NO_3 was included in the model. Higher P release was positively associated with TEP, and the ratio of Amox- P:NaOH P. These patterns suggest that soil P, particularly that bound to amorphous Al and Fe (Amox-extractable), is more likely to be released to the water column than P bound to crystalline Al and Fe. This is consistent with findings that increased crystallinity led to a loss in sorption capacity and in turn P release after reflooding (Schönbrunner et al., 2012). Variables negatively correlated with P release included total extractable Al, clay, the ratio of amorphous P: amorphous metals, and HCl-extractable SRP. Al

can act as a sorption site, P bound to amorphous Al is more easily sorbed than crystalline Al P (Weihrauch & Opp, 2018) which may explain why amorphous P:crystalline P predicts P release, while total extractable aluminum is negatively correlated with P release. Further, the amorphous P: amorphous metals accounts for amorphous Fe in addition to Al, which can be more redox sensitive (Darke & Walbridge, 2000) leading to greater P release once redox conditions change.

After 8 days of flooding, predictors of P release in cores that had undergone FT included soil characteristics that were positively associated with P release (Amox-P:NaOH-extractable P, DCB-SRP, and HCl- SRP) and those that were negatively correlated with P release (NaOH- NRP, Amox-P:Amox Al + Fe, and sand). Higher water column NO_3 predicted more P release, while higher water column pH was associated with less P. Opposite patterns in pH and HCl-SRP could represent reductions in pH that led to the dissolution of Ca-bound P, as Ca-P minerals are more soluble with lower pH (Weihrauch & Opp, 2019). This contrasts from 4-day P release models in FT cores where HCl-SRP was associated with P retention, suggesting Ca sorption sites became saturated. In addition, DCB-SRP associated with the redox sensitive P pool was likely being released simultaneously as shown by the positive relationship with P release. The release of redox-sensitive P is usually associated with increases in pH (Gu et al., 2019), which are present on average between 4 and 8-days of flooding in FT cores but no other timepoints. This may suggest that both Ca and redox sensitive pools are important at this time. Many have found that soils are either dominated by Ca-P dynamics in alkaline soils (Amarawansa et al., 2015; Jayarathne et al., 2016). or redox sensitive P pools in more acidic soils (Shenker et al., 2005), so the influence of both throughout the flood incubation is interesting. The relationship between NaOH-extractable NRP and reduced P release is somewhat surprising, as the pool is usually associated with organic-P which can be released to the water column during flooding from the microbial P pool or other organic sources. A study by Yevdokimov et al. (2016) found that disturbances like drying-rewetting and FT led to mobilization of microbial P more than other extractable P pools, but microbial recovery happened more rapidly under drying-wetting conditions due to warmer water temperatures (22°C vs 4°C). Our floodwater was maintained at 20°C in both treatments, which may have enabled the reuptake of initially released organic P by recovering microbial populations in both treatments. Though measurements of microbial P were not available, so the dynamics are not clear. The positive relationship of NO_3 and P in the water column may further support the idea that microbial uptake

of nutrients is occurring in treatment cores with less P release, as microbes tend to remove NO_3 from the water column.

Patterns in unfrozen cores showed a negative relationship between the HCl-SRP in soil and P release, but TEP predicted release, implying P release was driven by other extractable P pools. This coincides with the findings that HCl-extractable P in soil did not change significantly with 21 days of flooding (Figure 4). Following FT treatment, the HCl-SRP pool along with the DCB-SRP pools are predictive of P release at 8 days. Four days prior, like unfrozen cores 8 days into flooding, HCl-SRP was predictive of P retention and TEP of P release, which suggests the drivers of P release are different between treatments and dependent on the duration of the flooding. It is possible that P released from the soil or biomass early on was cycled back into other forms of P as evidenced by the increase in TEP following flooding in both treatment soils (Figure 4). While treatment differences existed in 8-day P release models, patterns in the ratios of Amox-P: NaOH P (amorphous: crystalline) and Amox-P: Amox- Al + Fe on P release in FT treatment core models mirrored the positive and negative trends seen in the unfrozen core models. This suggests that amorphous metal bound (Amox) P release may not be strongly influenced by FT. The large number of variables included in both models suggest the drivers of P release during flooding in these settings are complex and dependent on both soil and overlying water chemistry.

Lower HCl-SRP was measured in FT treatment cores post flooding compared to pre-flood soils and unfrozen cores post flooding. There was also a positive relationship between HCl-SRP and P release at 8, and 14 days of flooding. Together these suggest the Ca-bound P pool was strongly influenced by soil freezing prior to flooding. Interestingly, this pool did not change with freezing alone as evidenced by similar pool sizes from experiment 1. This suggests an interactive effect of freezing and flooding that could have been due to both the overlying water chemistry and differences in other soil P pools as evidenced by the models. Lower P concentrations in water at the onset of flooding in FT treated cores could have influenced patterns. Phosphorus released from other pools (TEP, amorphous Al-P) early on in flooding could be bound as Ca-P within the soil. Immobilization of P by Ca, and eventual precipitation has been documented in other temperate floodplain soils (Arenberg et al., 2020) and calcareous wetland soils (Shenker et al., 2005). This retention mechanism was evidenced by the inverse relationship between HCl-SRP and P release after 4 days, but not at any later time points in both unfrozen and FT cores. A possible explanation

is that as the soil became saturated with this pool, concentration gradients between the soil and water could have led to the dissolution of Ca-P. This could have been further promoted by the hydrologic conditions in experimental cores, which had a static hydraulic head that can promote diffusion of P from the soil to overlying surface water (Reddy et al., 2005). A study by Jayarathne et al. (2016) looking at P release to floodwater in calcareous soils found that concentrations of Ca and Mg corresponded with increased P and were likely due to the use of reverse osmosis water that led to dissolution from the pore water. Low floodwater nutrient concentrations may lead to Ca-P dissolution as a more common mechanism for P release compared to flooding with more nutrient rich water. Incoming flood water concentrations will be largely dependent on the timing of flooding following spring thaw, as seen in our water samples taken one week apart.

14 days

Unfrozen flooded cores showed steady increases in mean P release between 8 and 14 days of flooding. The highest P concentrations were largely associated with soil characteristics (DCB-SRP, HCl-SRP, NaOH-NRP, Amox-P: NaOH-P) and water chemistry (DO, and temperature). Lower P concentrations were predicted by soil characteristics (Amox-Al, sand, and TEP) along with floodwater (DOC, NO₃, and pH). The inclusion of many variables suggest the P release dynamics are complex, which is evidenced by the high variability in P release (Figure 6) where some cores are showing net removal of P from floodwater, while others are releasing P. The negative relationship between TEP, but positive relationship with several of the extractable P pools, might be the result of P cycling between the soil and overlying water as P bound to redox sensitive DCB-SRP, Ca-bound HCl-SRP, and organic NaOH-NRP pools are released, they can be recycled to other pools like amorphous Amox-Al. This is consistent with other findings under anaerobic conditions where P released from reduced Fe-oxides is partially sorbed to other redox-stable soil pools (Hoffmann et al., 2009; Darke & Walbridge, 2000). The transfer of P from redox sensitive P to other P pools is further evidenced by changes in the extractable P pools observed post-flooding (Figure 4). Again, lower DOC and NO₃ were associated with less P release providing evidence that microbial processes might be playing a role, as denitrification by microbes can remove these nutrients from the water column in floodplains (Baldwin & Mitchell, 2000). Warmer temperatures and higher DO, conditions that are good for microbial growth also positively predicted P release at this time point. All of the possible water chemistry variables were included

in the model, implying a strong interaction between overlying water chemistry and pre-flooding soil characteristics on P release.

Cores that underwent FT before flooding appeared to reach maximum P release 14 days into the 21-day flood incubation. Unlike control cores, FT treatment cores rarely showed net uptake of P two weeks after the onset of flooding and appeared to be controlled more by soil characteristics than water chemistry. Total extractable Fe, HCl-extractable P, and amorphous aluminum in baseline soils combined with floodwater DOC were associated with greater P release after 2 weeks of flooding. Retention of P was influenced by sand, NaOH-extractable NRP, and the ratio of amorphous (Amox-extractable) P:amorphous (Amox-extractable) Al + Fe. These patterns are similar to the drivers of P release 8 days into flooding in the same cores, however there are fewer water chemistry variables and total extractable Fe and redox sensitive DCB-SRP emerge as new predictors of P release, while the ratio of amorphous P: crystalline P is no longer included. Dissolved oxygen decreased between 8 days and 14 days of flooding, low DO promotes microbes to use Fe as an electron acceptor, liberating previously sorbed P (Reddy et al., 2000), which may explain the emergence of the redox sensitive pools as new drivers of P release at this time.

1.6 Conclusions

Experimental freeze-thaw treatment of intact floodplain soil cores generated meaningful differences in the different pools of P in floodplain soils and P released throughout a simulated 21-day flood. Freezing and thawing lead to changes in the distribution of P within different soil pools, as evidenced by reduction in organic SRP and increase in redox sensitive SRP following an experimental FT cycle (Experiment 1). Flooding, of both unfrozen and FT treatments, led to further changes in the amount of total extractable soil P and its distribution into the different soil P pools (Experiment 2). Greater pools of organic P post-flooding in FT treated cores compared to unfrozen cores post-flooding could have been due to increases in the biomass present in soil post FT due to lysis of microbial or plant biomass and other organic P pools. However, based on the consistent negative relationship between the organic P pool in pre-flood baseline soils and P released throughout the FT flood, the association of this pool with greater P release following FT was not well supported.

While on average, unfrozen cores released P, it appeared the dynamics between release and uptake were more complex after a longer period of flooding compared to FT cores as evidenced by lower model R^2 values at every timepoint, except for 14 days where 5 additional variables were included and only produced marginally better results compared to FT cores. Interactive effects of FT and flooding may exist, as post-flooding clay bound/Al-oxide exchangeable P and organic P pools were higher in FT treatment cores while Ca-P was lower compared to post-flooding unfrozen soils. Differences in starting water chemistry may have played a role in the observed patterns of P release and contributed to the more complex dynamics in unfrozen cores. Water collected for unfrozen incubations had greater nutrient concentrations compared to water collected for FT treatment cores which had undetectable amounts of P. Differences between soil solution P and overlying water may have exacerbated the influence of Ca-P in cores flooded after FT, as concentration gradients can lead to dissolution. The positive correlation of Ca-P and negative correlation of pH on P release 14 days into flooding of unfrozen cores mirrors patterns observed in FT treatment cores at 8 days, suggesting FT treatment or starting water chemistry also impacted the timing of P release associated with this pool. The influence of both metal-bound and Ca-P throughout flooding in both treatments was interesting, as P release is usually dominated by one or the other depending on the soil type.

These results provide important insights to the potential physical and chemical dynamics of agricultural and restored floodplain soils. Upon flooding, all soils on average released P to the overlying water column and soils that underwent freezing released even larger amounts. Findings from this study also support the idea that P pools will change following FT in floodplains, these changes may influence the mechanisms controlling P release during flooding, which is important to making informed management decisions. If redox sensitive P pools increase with freezing as seen here, designing floodplains with shorter inundation times might prevent the prevalence of reducing conditions that can liberate P. Further research investigating changes in extractable P pools after repeated FT cycles would be beneficial to better maximize restoration design and management by improving our understanding of P dynamics across the entire winter season before spring melt and flooding.

APPENDIX A. PHOSPHORUS EXTRACTION SCHEME

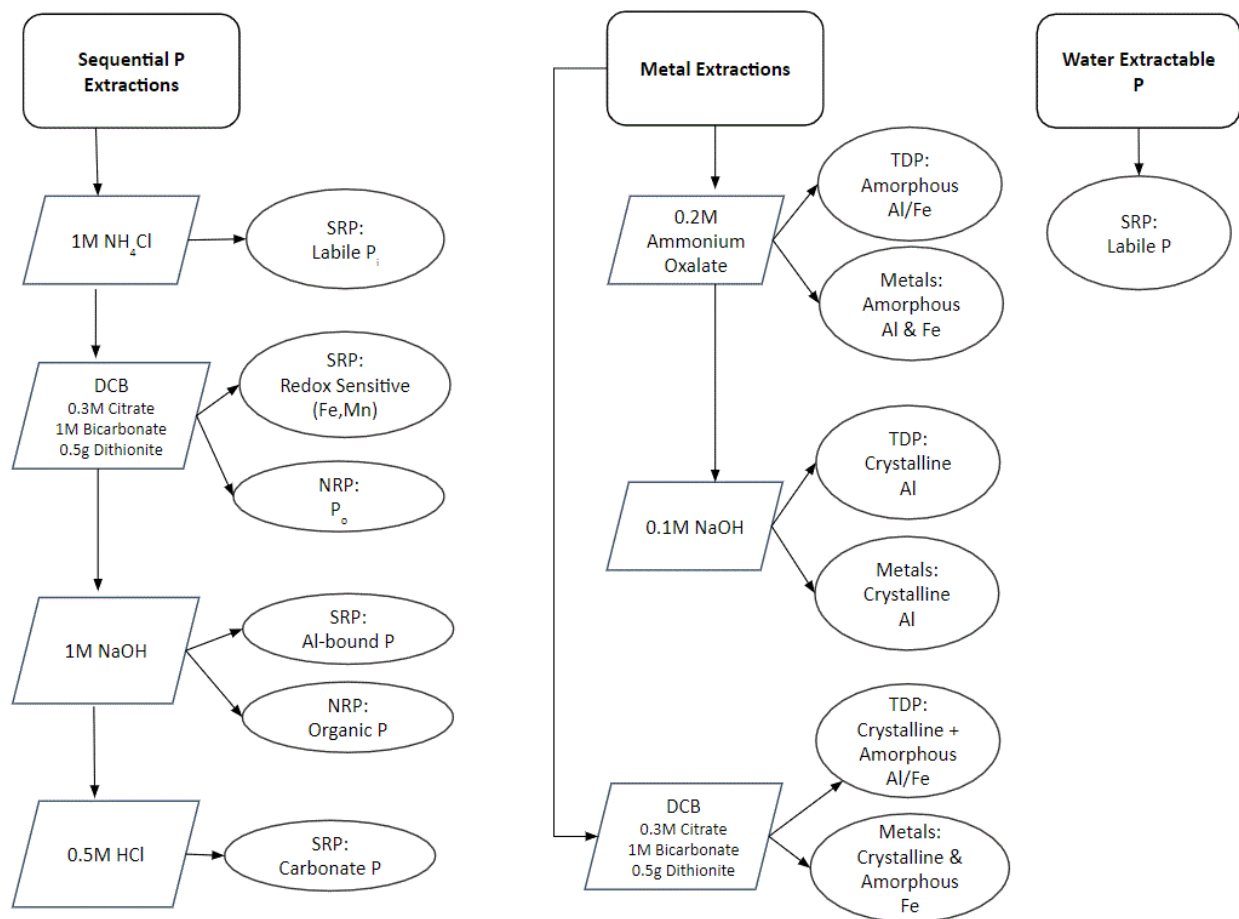
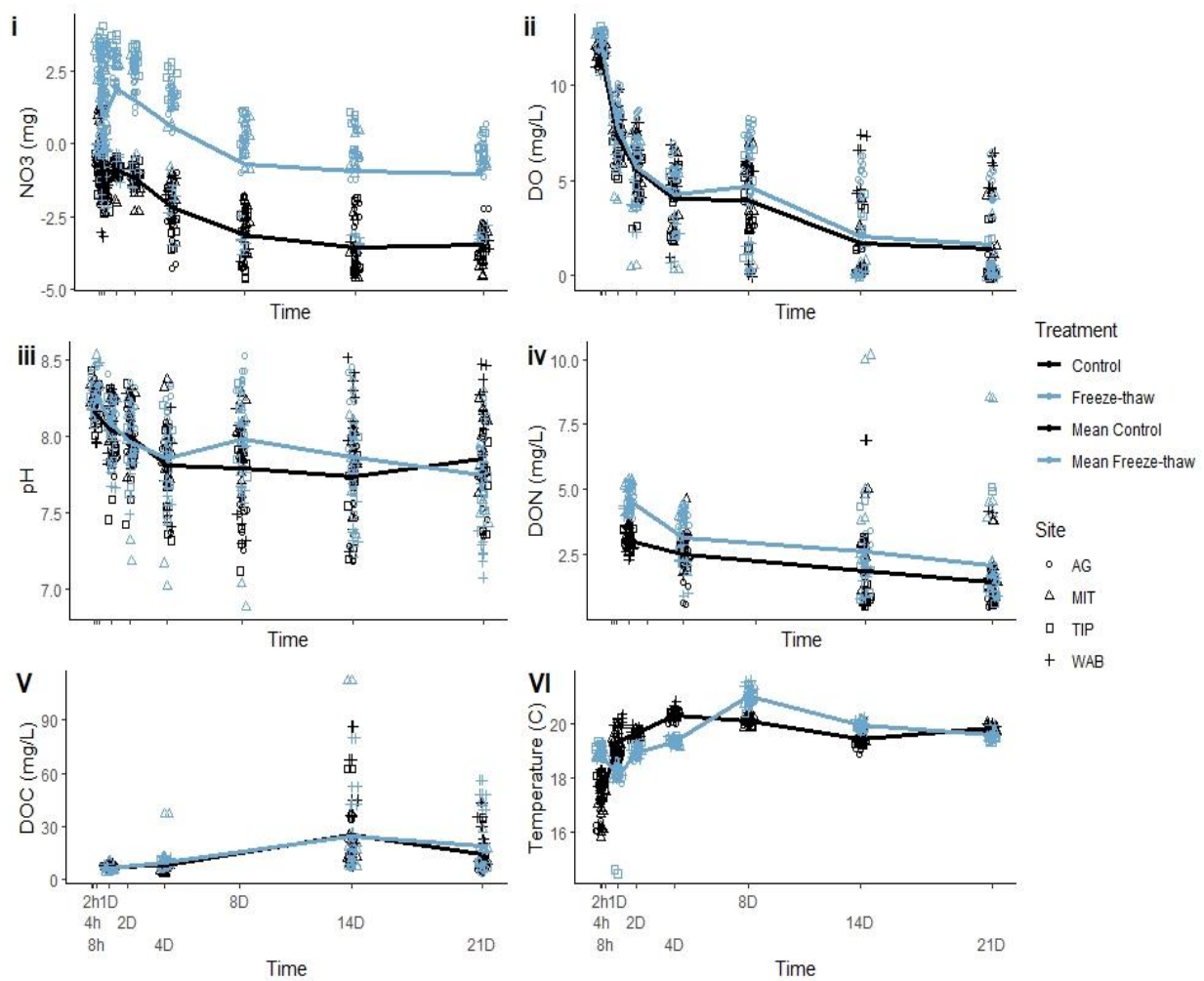


Figure A. 1 Sequential extraction schemes used throughout experiment.

APPENDIX B. SUPPLEMENTAL DATA

B. Table 1- mean extractable soil P and metals from all sites split by their respective treatment.

<u><i>Variable</i></u> <u><i>(mg g⁻¹ soil)</i></u>	<u><i>Exp 1 Control</i></u>	<u><i>Exp 1 Frozen</i></u>	<u><i>Exp 2 Baseline</i></u>	<u><i>Exp 2 Control</i></u>	<u><i>Exp 2 Frozen</i></u>
<i>NH₄Cl-SRP</i>	0.00 (±0.00)	0.001 (± 0.003)	0.00 (±0.00)	0.00 (±0.00)	0.00 (±0.00)
<i>NaOH-SRP</i>	0.09 (± 0.06)	0.06 (± 0.02)	0.05 (± 0.02)	0.06 (± 0.03)	0.07 (± 0.05)
<i>NaOH-NRP</i>	0.10 (± 0.05)	0.09 (± 0.04)	0.10 (± 0.05)	0.06 (± 0.06)	0.13 (±0.07)
<i>DCB-SRP</i>	0.41 (± 0.18)	0.52 (± 0.25)	0.33 (± 0.21)	0.70 (± 0.32)	0.56 (± 0.28)
<i>HCl-SRP</i>	0.10 (± 0.05)	0.08 (± 0.03)	0.17 (± 0.05)	0.37 (± 0.13)	0.23 (± 0.12)
<i>T. Ext. P</i>	0.70 (±0.22)	0.75 (±0.29)	0.66 (± 0.26)	1.18 (± 0.40)	1.01 (± 0.42)
<i>Amox-Al</i>	0.85 (±0.29)	0.76 (±0.29)	0.77 (± 0.26)	0.75 (± 0.31)	0.77 (± 0.22)
<i>Amox-Fe</i>	2.87 (± 0.99)	2.60 (± 0.99)	2.66 (± 0.95)	2.95 (± 1.38)	3.15 (± 1.13)
<i>Amox-Mn</i>	0.42 (± 0.16)	0.42 (± 0.16)	0.42 (± 0.14)	0.38 (± 0.16)	0.37 (± 0.16)
<i>Amox-P</i>	0.35 (± 0.11)	0.32 (± 0.11)	0.33 (± 0.14)	0.32 (± 0.15)	0.32 (± 0.13)
<i>NaOH-Al</i>	0.32 (± 0.20)	0.23 (± 0.16)	0.23 (± 0.12)	0.19 (± 0.16)	0.15 (± 0.11)
<i>NaOH-Fe</i>	0.23 (± 0.11)	0.18 (± 0.13)	0.20 (± 0.11)	0.14 (± 0.12)	0.10 (± 0.08)
<i>NaOH-Mn</i>	0.006 (± 0.005)	0.002 (± 0.001)	0.006 (± 0.01)	0.003 (± 0.003)	0.003 (± 0.002)
<i>NaOH-P</i>	0.11 (± 0.04)	0.04 (± 0.05)	0.04 (± 0.02)	0.04 (± 0.02)	0.03 (± 0.02)
<i>T. Ext. Fe</i>	7.11 (± 2.35)	6.92 (± 1.66)	7.10 (± 2.14)	6.13 (± 2.37)	6.16 (± 1.71)
<i>T. Ext Al</i>	1.18 (± 0.44)	0.99 (± 0.42)	1.00 (± 0.35)	0.95 (± 0.44)	0.92 (± 0.31)



B Figure 1- Water chemistry throughout the 21-day flood incubation where graph i.NO₃ mg; ii. DO mg L⁻¹; iii. pH ; iv. DON mg L⁻¹; V. DOC mg L⁻¹; VI Temperature °C. Ag = Wabash R. Agriculture site; Mit = Wabash R. Mitigation site; Tip = Tippecanoe R. Prairie

REFERENCES

- Aldous, A., McCormick, P., Ferguson, C., Graham, S., & Craft, C. (2005). Hydrologic regime controls soil phosphorus fluxes in restoration and undisturbed wetlands. In *Restoration Ecology* (Vol. 13, Issue 2). <https://doi.org/10.1111/j.1526-100X.2005.00043.x>
- Amarawansha, E. A. G. S., Kumaragamage, D., Flaten, D., Zvomuya, F., & Tenuta, M. (2015). Phosphorus Mobilization from Manure-Amended and Unamended Alkaline Soils to Overlying Water during Simulated Flooding. *Journal of Environmental Quality*, 44(4), 1252–1262. <https://doi.org/10.2134/jeq2014.10.0457>
- Arenberg, M. R., & Arai, Y. (2019). Uncertainties in soil physicochemical factors controlling phosphorus mineralization and immobilization processes. In *Advances in Agronomy* (1st ed., Vol. 154). Elsevier Inc. <https://doi.org/10.1016/bs.agron.2018.11.005>
- Baldwin, D. S., & Mitchell, A. M. (2000). The effects of drying and re-flooding on the sediment and soil nutrient dynamics of lowland river–floodplain systems: a synthesis. *Regulated Rivers: Research & Management*, 16(5), 457–467. [https://doi.org/10.1002/1099-1646\(200009/10\)16:5<457::aid-rrr597>3.3.co;2-2](https://doi.org/10.1002/1099-1646(200009/10)16:5<457::aid-rrr597>3.3.co;2-2)
- Bechmann, M. E., Kleinman, P. J. A., Sharpley, A. N., & Saporito, L. S. (2005). Freeze-Thaw Effects on Phosphorus Loss in Runoff from Manured and Catch-Cropped Soils. *Journal of Environmental Quality*, 34(6), 2301–2309. <https://doi.org/10.2134/jeq2004.0415>
- Bennett, E. M., & Schipanski, M. E. (2012). The phosphorus cycle. *Fundamentals of Ecosystem Science*, 159–178. <https://doi.org/10.1016/b978-0-08-091680-4.00008-1>
- Blackwell, M. S. A., Brookes, P. C., de la Fuente-Martinez, N., Gordon, H., Murray, P. J., Snars, K. E., Williams, J. K., Bol, R., & Haygarth, P. M. (2010). Phosphorus Solubilization and Potential Transfer to Surface Waters from the Soil Microbial Biomass Following Drying–Rewetting and Freezing–Thawing (pp. 1–35). [https://doi.org/10.1016/s0065-2113\(10\)06001-3](https://doi.org/10.1016/s0065-2113(10)06001-3)
- Casson, N. J., Wilson, H. F., & Higgins, S. M. (2019). Hydrological and Seasonal Controls of Phosphorus in Northern Great Plains Agricultural Streams. *Journal of Environmental Quality*, 48(4), 978–987. <https://doi.org/10.2134/jeq2018.07.0281>
- Cober, J. R., Macrae, M. L., & Van Eerd, L. L. (2019). Winter Phosphorus Release from Cover Crops and Linkages with Runoff Chemistry. *Journal of Environmental Quality*, 48(4), 907–914. <https://doi.org/10.2134/jeq2018.08.0307>
- Champely, S. (2020). pwr: Basic Functions for Power Analysis. R package version 1.3-0. <https://CRAN.R-project.org/package=pwr>

- Cohen, J. (2013). *Statistical Power Analysis for the Behavioral Sciences*. Statistical Power Analysis for the Behavioral Sciences. <https://doi.org/10.4324/9780203771587>
- Darke, A. K., & Walbridge, M. R. (1994). Estimating non-crystalline and crystalline aluminum and iron by selective dissolution in a riparian forest soil1. *Communications in Soil Science and Plant Analysis*, 25(11–12), 2089–2101. <https://doi.org/10.1080/00103629409369174>
- Filippelli, G. M. (2019). The global phosphorus cycle. *Phosphates: Geochemical, Geobiological and Materials Importance*, 48, 391–426. <https://doi.org/10.2138/rmg.2002.48.10>
- Fitzhugh, R. D., Driscoll, C. T., Groffman, P. M., Tierney, G. L., Fahey, T. J., & Hardy, J. P. (2001). Effects of soil freezing disturbance on soil solution nitrogen, phosphorus, and carbon chemistry in a northern hardwood ecosystem. In *Biogeochemistry* (Vol. 56).
- Freppaz, M., Williams, B. L., Edwards, A. C., Scalenghe, R., & Zanini, E. (2007). Simulating soil freeze/thaw cycles typical of winter alpine conditions: Implications for N and P availability. *Applied Soil Ecology*, 35(1), 247–255. <https://doi.org/10.1016/j.apsoil.2006.03.012>
- Gao, D., Zhang, L., Liu, J., Peng, B., Fan, Z., Dai, W., Jiang, P., & Bai, E. (2018). Responses of terrestrial nitrogen pools and dynamics to different patterns of freeze-thaw cycle: A meta-analysis. *Global Change Biology*, 24(6), 2377–2389. <https://doi.org/10.1111/gcb.14010>
- Gu, S., Gruau, G., Dupas, R., Petitjean, P., Li, Q., & Pinay, G. (2019). Respective roles of Fe-oxyhydroxide dissolution, pH changes and sediment inputs in dissolved phosphorus release from wetland soils under anoxic conditions. *Geoderma*, 338, 365–374. <https://doi.org/10.1016/j.geoderma.2018.12.034>
- Hadley Wickham, Romain François, Lionel Henry and Kirill Müller (2021). dplyr: A Grammar of Data Manipulation. R package version 1.0.3. <https://CRAN.R-project.org/package=dplyr>
- Hebbali, A. (2020). olsrr: Tools for Building OLS Regression Models. R package version 0.5.3. <https://CRAN.R-project.org/package=olsr>
- Heiri, O., Lotter, A. F., & Lemcke, G. (2001). *Loss on ignition as a method for estimating organic and carbonate content in sediments : reproducibility and comparability of results*. 101–110.
- Helsel, D. R., Hirsch, R. M., Ryberg, K. R., Archfield, S. A., & Gilroy, E. J. (2020). Statistical methods in water resources: U.S. Geological Survey Techniques and Methods, book 4, chapter A3. *Book 4, Hydrologic Analysis and Interpretation*, 1–484. <https://doi.org/10.3133/tm4A3>
- Henry, H. A. L. (2007). Soil freeze-thaw cycle experiments: Trends, methodological weaknesses and suggested improvements. *Soil Biology & Biochemistry*, 39, 977–986. <https://doi.org/10.1016/j.soilbio.2006.11.017>

- Henry, H. A. L. (2008). Climate change and soil freezing dynamics: Historical trends and projected changes. *Climatic Change*, 87(3–4), 421–434. <https://doi.org/10.1007/s10584-007-9322-8>
- Jayarathne, P. D. K. D., Kumaragamage, D., Indraratne, S., Flaten, D., & Goltz, D. (2016). Phosphorus Release to Floodwater from Calcareous Surface Soils and Their Corresponding Subsurface Soils under Anaerobic Conditions. *Journal of Environmental Quality*, 45(4), 1375–1384. <https://doi.org/10.2134/jeq2015.11.0547>
- Junk, W. J., Bayley, P. B., & Sparks, R. E. (1989). the Flood Pulse Concept in River-Flooding Systems. *Canadian Special Publication of Fisheries and Aquatic Sciences*, September, 110–127.
- King, K. W., Williams, M. R., Macrae, M. L., Fausey, N. R., Frankenberger, J., Smith, D. R., Kleinman, P. J. A., & Brown, L. C. (2015). Phosphorus Transport in Agricultural Subsurface Drainage: A Review. *Journal of Environmental Quality*, 44(2), 467–485. <https://doi.org/10.2134/jeq2014.04.0163>
- Kumaragamage, D., Concepcion, A., Gregory, C., Goltz, D., Indraratne, S., & Amarawansa, G. (2020). Temperature and freezing effects on phosphorus release from soils to overlying floodwater under flooded-anaerobic conditions. *Journal of Environmental Quality*, 49(3), 700–711. <https://doi.org/10.1002/jeq2.20062>
- Liu, J., Baulch, H. M., Macrae, M. L., Wilson, H. F., Elliott, J. A., Bergström, L., Glenn, A. J., & Vadas, P. A. (2019). Agricultural Water Quality in Cold Climates: Processes, Drivers, Management Options, and Research Needs. *Journal of Environmental Quality*, 48(4), 792–802. <https://doi.org/10.2134/jeq2019.05.0220>
- Lumley, T based on Fortran code by Alan Miller (2020). leaps: Regression Subset Selection. R package version 3.1. <https://CRAN.R-project.org/package=leaps>
- Matzner, E., & Borken, W. (2008). Do freeze-thaw events enhance C and N losses from soils of different ecosystems? A review. *European Journal of Soil Science*, 59(2), 274–284. <https://doi.org/10.1111/j.1365-2389.2007.00992.x>
- McMillan, S. K., & Noe, G. B. (2017). Increasing floodplain connectivity through urban stream restoration increases nutrient and sediment retention. *Ecological Engineering*, 108(August), 284–295. <https://doi.org/10.1016/j.ecoleng.2017.08.006>
- Messiga, A. J., Ziadi, N., Morel, C., & Parent, L.-E. (2010). Soil phosphorus availability in no-till versus conventional tillage following freezing and thawing cycles. *Canadian Journal of Soil Science*, 90(3), 419–428. <https://doi.org/10.4141/cjss09029>
- Midwestern Regional Climate Center. (2020). (1981-2010) Temperature summary for station USW00014835. Retrieved from:

https://mrcc.illinois.edu/mw_climate/climateSummaries/climSummOut_temp.jsp?stnId=USW00014835

- Mohanty, S. K., Saiers, J. E., & Ryan, J. N. (2014). Colloid-facilitated mobilization of metals by freeze-thaw cycles. *Environmental Science and Technology*, 48(2), 977–984.
<https://doi.org/10.1021/es403698u>
- NOAA. Climate Data Online. National Centers for Environmental Information website,
<https://www.ncdc.noaa.gov/cdo-web/> accessed on 4/5/2021.
- Noe, G. B., Boomer, K., Gillespie, J. L., Hupp, C. R., Martin-Alciati, M., Floro, K., Schenk, E. R., Jacobs, A., & Strano, S. (2019). The effects of restored hydrologic connectivity on floodplain trapping vs. release of phosphorus, nitrogen, and sediment along the Pocomoke River, Maryland USA. *Ecological Engineering*, 138, 334–352.
<https://doi.org/10.1016/j.ecoleng.2019.08.002>
- Noe, G. B., & Hupp, C. R. (2007). Seasonal variation in nutrient retention during inundation of a short-hydroperiod floodplain. *River Research and Applications*, 23(10), 1088–1101.
<https://doi.org/10.1002/rra.1035>
- Pacini, N., & Gächter, R. (1999). Speciation of riverine particulate phosphorus during rain events. In *Biogeochemistry* (Vol. 47).
- Pease, L. A., King, K. W., Williams, M. R., LaBarge, G. A., Duncan, E. W., & Fausey, N. R. (2018). Phosphorus export from artificially drained fields across the Eastern Corn Belt. *Journal of Great Lakes Research*, 44(1), 43–53. <https://doi.org/10.1016/j.jglr.2017.11.009>
- Plach, J., Puer, W., Macrae, M., Kompanizare, M., McKague, K., Carlow, R., & Brunke, R. (2019). Agricultural Edge-of-Field Phosphorus Losses in Ontario, Canada: Importance of the Nongrowing Season in Cold Regions. *Journal of Environmental Quality*, 48(4), 813–821. <https://doi.org/10.2134/jeq2018.11.0418>
- Reddy K.R., D. A. E. D. y W. . H. (2000). Biogeochem of wetlands.pdf. In *CRC press. Handbook of Soil Science* (pp. G89-119).
- Royer, T. V., David, M. B., & Gentry, L. E. (2006). Timing of riverine export of nitrate and phosphorus from agricultural watersheds in Illinois: Implications for reducing nutrient loading to the Mississippi River. *Environmental Science and Technology*, 40(13), 4126–4131. <https://doi.org/10.1021/es052573n>
- Satchithanantham, S., English, B., & Wilson, H. (2019). Seasonality of Phosphorus and Nitrate Retention in Riparian Buffers. *Journal of Environmental Quality*, 48(4), 915–921.
<https://doi.org/10.2134/jeq2018.07.0280>

- Schönbrunner, I. M., Preiner, S., & Hein, T. (2012). Impact of drying and re-flooding of sediment on phosphorus dynamics of river-floodplain systems. *Science of the Total Environment*, 432, 329–337. <https://doi.org/10.1016/j.scitotenv.2012.06.025>
- Sharma, S., Szele, Z., Schilling, R., Munch, J. C., & Schloter, M. (2006). Influence of Freeze-Thaw Stress on the Structure and Function of Microbial Communities and Denitrifying Populations in Soil. *Appl. Environ. Microbiol.*, 72(3), 2148–2154. <https://doi.org/10.1128/AEM.72.3.2148-2154.2006>
- Shenker, M., Seitelbach, S., Brand, S., Haim, A., & Litaor, M. I. (2005). Redox reactions and phosphorus release in re-flooded soils of an altered wetland. *European Journal of Soil Science*, 56(4), 515–525. <https://doi.org/10.1111/j.1365-2389.2004.00692.x>
- Smeck, N. E. (1985). Phosphorus dynamics in soils and landscapes. *Geoderma*, 36(3–4), 185–199. [https://doi.org/10.1016/0016-7061\(85\)90001-1](https://doi.org/10.1016/0016-7061(85)90001-1)
- Smith, A. S., & Jacinthe, P. A. (2014). A mesocosm study of the effects of wet-dry cycles on nutrient release from constructed wetlands in agricultural landscapes. *Environmental Sciences: Processes and Impacts*, 16(1), 106–115. <https://doi.org/10.1039/c3em00465a>
- Song, Y., Zou, Y., Wang, G., & Yu, X. (2017). Altered soil carbon and nitrogen cycles due to the freeze-thaw effect: A meta-analysis. *Soil Biology and Biochemistry*, 109, 35–49. <https://doi.org/10.1016/j.soilbio.2017.01.020>
- Soil Survey Staff, Natural Resources Conservation Service, United States Department of Agriculture. Web Soil Survey. Available online at the following link: <http://websoilsurvey.sc.egov.usda.gov/>. Accessed 19 Oct 2019.
- Sun, D., Yang, X., Wang, C., Hao, X., Hong, J., & Lin, X. (2019). Dynamics of available and enzymatically hydrolysable soil phosphorus fractions during repeated freeze-thaw cycles. *Geoderma*, 345(July), 1–4. <https://doi.org/10.1016/j.geoderma.2019.03.009>
- Surridge, B. W. J., Heathwaite, A. L., & Baird, A. J. (2012). Phosphorus mobilisation and transport within a long-restored floodplain wetland. *Ecological Engineering*, 44, 348–359. <https://doi.org/10.1016/j.ecoleng.2012.02.009>
- Tockner, K., Pennetzdorfer, D., Reiner, N., Schiemer, F., & Ward, J. V. (1999). Hydrological connectivity, and the exchange of organic matter and nutrients in a dynamic river-floodplain system (Danube, Austria). *Freshwater Biology*, 41(3), 521–535. <https://doi.org/10.1046/j.1365-2427.1999.00399.x>
- Van Esbroeck, C. J., Macrae, M. L., Brunke, R. R., & McKague, K. (2016). Surface and subsurface phosphorus export from agricultural fields during peak flow events over the nongrowing season in regions with cool, temperate climates. *Journal of Soil and Water Conservation*, 72(1), 65–76. <https://doi.org/10.2489/jswc.72.1.65>

- Vaz, M. D. R., Edwards, A. C., Shand, C. A., & Cresser, M. S. (1994). Changes in the chemistry of soil solution and acetic-acid extractable P following different types of freeze/thaw episodes. *European Journal of Soil Science*, 45(3), 353–359. <https://doi.org/10.1111/j.1365-2389.1994.tb00519.x>
- Weihrauch, C., & Opp, C. (2018). Ecologically relevant phosphorus pools in soils and their dynamics: The story so far. *Geoderma*, 325(February), 183–194. <https://doi.org/10.1016/j.geoderma.2018.02.047>
- Williams, M. R., King, K. W., Baker, D. B., Johnson, L. T., Smith, D. R., & Fausey, N. R. (2016). Hydrologic and biogeochemical controls on phosphorus export from Western Lake Erie tributaries. *Journal of Great Lakes Research*, 42(6), 1403–1411. <https://doi.org/10.1016/j.jglr.2016.09.009>
- Wright, R. B., Lockaby, B. G., & Walbridge, M. R. (2001). Phosphorus Availability in an Artificially Flooded Southeastern Floodplain Forest Soil. *Soil Science Society of America Journal*, 65(4), 1293–1302. <https://doi.org/10.2136/sssaj2001.6541293x>
- Xu, G., Sun, J. N., Xu, R. F., Lv, Y. C., Shao, H. B., Yan, K., Zhang, L. H., & Blackwell, M. S. A. (2011). Effects of air-drying and freezing on phosphorus fractions in soils with different organic matter contents. *Plant, Soil and Environment*, 57(5), 228–234. <https://doi.org/10.17221/428/2010-pse>
- Yevdokimov, I., Larionova, A., & Blagodatskaya, E. (2016). Microbial immobilisation of phosphorus in soils exposed to drying-rewetting and freeze-thawing cycles. *Biology and Fertility of Soils*, 52(5), 685–696. <https://doi.org/10.1007/s00374-016-1112-x>
- Zhang, Z., Ma, W., Feng, W., Xiao, D., & Hou, X. (2016). Reconstruction of Soil Particle Composition During Freeze-Thaw Cycling: A Review. In *Pedosphere* (Vol. 26, Issue 2, pp. 167–179). Institute of Soil Science. [https://doi.org/10.1016/S1002-0160\(15\)60033-9](https://doi.org/10.1016/S1002-0160(15)60033-9)